Instrumentation and Modeling of the North 140 Section of Magmont Mine, Bixby, MO

By D. R. Tesarik and R. W. McKibbin

Mission: As the Nation's principal conservation agency, the Department of the Interior has responsibility for most of our nationally-owned public lands and natural and cultural resources. This includes fostering wise use of our land and water resources, protecting our fish and wildlife, preserving the environmental and cultural values of our national parks and historical places, and providing for the enjoyment of life through outdoor recreation. The Department assesses our energy and mineral resources and works to assure that their development is in the best interests of all our people. The Department also promotes the goals of the Take Pride in America campaign by encouraging stewardship and citizen responsibility for the public lands and promoting citizen participation in their care. The Department also has a major responsibility for American Indian reservation communities and for people who live in Island Territories under U.S. Administration.

Instrumentation and Modeling of the North 140 Section of Magmont Mine, Bixby, MO

By D. R. Tesarik and R. W. McKibbin

CONTENTS

ILLUSTRATIONS

ILLUSTRATIONS–Continued

Page

TABLES

UNIT OF MEASURE ABBREVIATIONS USED IN THIS REPORT

deg	degree	pcf	pound per cubic foot
ft	foot	psi	pound per square inch
h	hour	st	short ton
in	inch	yr	year

INSTRUMENTATION AND MODELING OF THE NORTH 140 SECTION OF MAGMONT MINE, BIXBY, MO

By D. R. Tesarik,[1] and R. W. McKibbin[2]

ABSTRACT

An instrumentation and numeric modeling study was conducted by the Bureau of Mines at the Magmont Mine in Bixby, MO. An isolated section of this room-and-pillar mine was monitored with borehole and closure extensometers during a pillar recovery program to determine stress redistribution. In situ stress measurements were taken in the rib before pillar extraction began. Sample cores from the boreholes were taken for analysis of the properties of the host rock in the laboratory. The extensometers recorded no measurable displacements during most of the operation.

Two-dimensional, finite-element; three-dimensional, finite-element; and three-dimensional displacement discontinuity codes were used to model the area of study. The finite-element models were run with two initial stress conditions, i.e., stress due to gravity only and stress obtained by in situ measurements. Horizontal stresses in the models reduced the calculated factor-of-safety in the mine back by up to a factor of 10, but did not have a significant effect on calculated pillar stability.

[1]Mathematician.
[2]Mining engineer.
Spokane Research Center, U.S. Bureau of Mines, Spokane, WA.

INTRODUCTION

As part of its research program in mining technology, the Bureau of Mines is examining techniques for mining with backfill. The objective is to incorporate mine backfill to minimize surface waste disposal effects, increase resource recovery, reduce surface subsidence, and improve mining efficiency. Mines currently using, or planning to use, backfill in their operations are candidates for study. The current work is directed toward monitoring the behavior of the North 140 section of Cominco American's Magmont Mine during pillar recovery operations. This area was originally planned to be totally filled with cycloned mill tailings as retreat mining took place, but the need for backfill in other areas of the mine resulted in a shortage of sand and the rooms were filled to only one-third their depths.

The geotechnical instrumentation consisted of the installation of two vertical borehole extensometers, three horizontal borehole extensometers, and two closure extensometers. In situ stress was evaluated in the rib to measure the virgin stress field. Cores from this work were used for analyzing material properties of the host rock.

Two-dimensional, finite-element; three-dimensional, finite-element; and three-dimensional displacement discontinuity models were used to evaluate the changes in the stress state as the pillar recovery program progressed. The objective was to calibrate the models by using displacement data from the extensometers and then to use the calibrated version of the models to predict the effect of further pillar extraction on mine stability. The relationship between the properties of the laboratory test specimens and the in-place rock is normally achieved by fitting a line to the measured displacements versus predicted displacements and then reducing the elastic moduli that are entered into the computer program by using the slope of the regression line. The strengths of the materials are generally reduced until the plastic zones produced by the model are similar in size and shape to those observed underground.

ACKNOWLEDGMENTS

The authors wish to express their appreciation to Cominco American Inc., Magmont Mines, Bixby, MO, and especially to W. K. Callaway, superintendent of engineering; K. D. Malone, superintendent of mines; and J. Hafner, senior mine engineer, for providing a location for this field work, providing equipment and assistance during instrument installation, maintaining the instruments and computer system during mining operations, and providing mine maps and geological information.

The authors also wish to thank W. G. Pariseau, professor, Department of Mining Engineering, University of Utah, Salt Lake City, UT, for providing the numeric modeling codes used in this work and assisting in their interpretation.

MAGMONT MINE

Cominco American's Magmont Mine is located 100 miles southwest of St. Louis in a deposit called the New Lead Belt or Viburnum Trend (fig. 1). The trend extends from the town of Viburnum and runs approximately 35 miles to the south. The east-west distance across the trend is approximately 2,000 ft. The deposit was discovered in 1955; in 1960, Dresser Industries, Inc., Houston, TX, and Cominco American Inc., Spokane, WA, began exploration. The deposit is primarily lead with marketable amounts of zinc, copper, and silver (1).[3]

Between 1965 and 1967, construction of surface facilities and shaft sinking took place. Limited production began in 1968, and full production began in 1971. Since then, the Magmont Mine has produced more than 1 million st/yr of ore (1).

A generalized stratigraphic column of the Magmont Mine (fig. 2) shows that the formations overlying the ore zone are primarily dolomite, with the exception of the Davis Shale 95 ft above the ore body. The ore lies approximately 1,000 ft below the surface. The thickness of the ore ranges from 10 ft in some areas to 90 ft in the North High Ore area (2). The area of this study is in the northwest section of the mine in the main ore horizon called the North 140, where the ore zone averages 25 ft.

The Magmont Mine uses a room-and-pillar mining method and trackless diesel equipment. Pillars are approximately 25 ft square and rooms are approximately 35 ft wide. Intersections and headings are bolted using 5-ft split sets or Swellex[4] bolts on 5-ft centers.

---

[3]Italic numbers in parentheses refer to items in the list of references preceding the appendix at the end of this report.

[4]Reference to specific products does not imply endorsement by the Bureau of Mines.

Figure 1.–Location map of New Lead Belt.

Surface

LEGEND

1,300

1,200

1,100

1,000

900

800

700

600

ELEVATION, ft

500

400

300

200

100

0

-100

-200

60-ft overburden

50-ft Gasconade Dolomite

195-ft Eminence Dolomite

350-ft Potosi Dolomite

110-ft Derby-Doerun Dolomite

150-ft Davis Formation

North High Ore

300-ft Bonneterre Formation

330-ft Lamotte Sandstone

Main ore horizon

Shaft bottom

Window ore

Sea level

Dolomite

Cherty dolomite

Dolomite with quartz druse in cavities

Argillaceous dolomite

Shale

Ore horizon

Sandstone

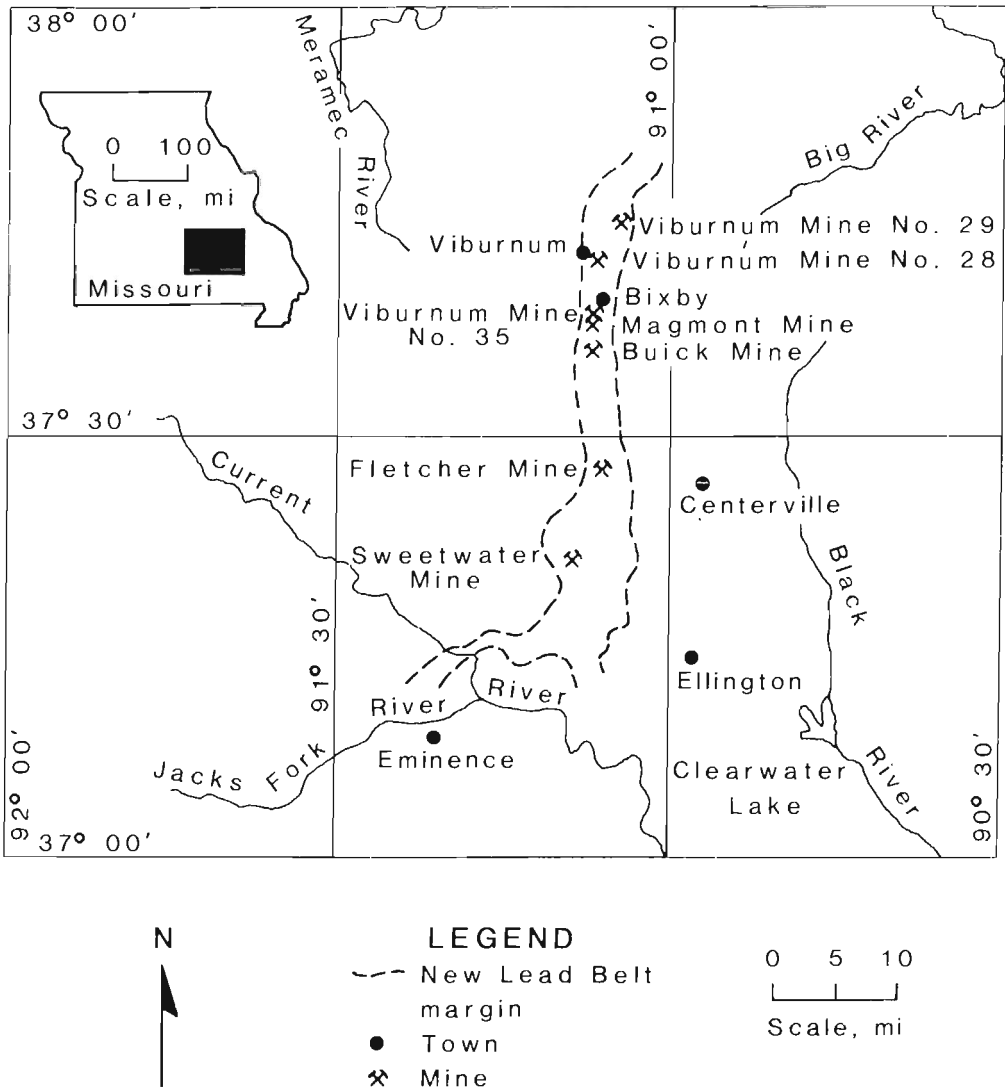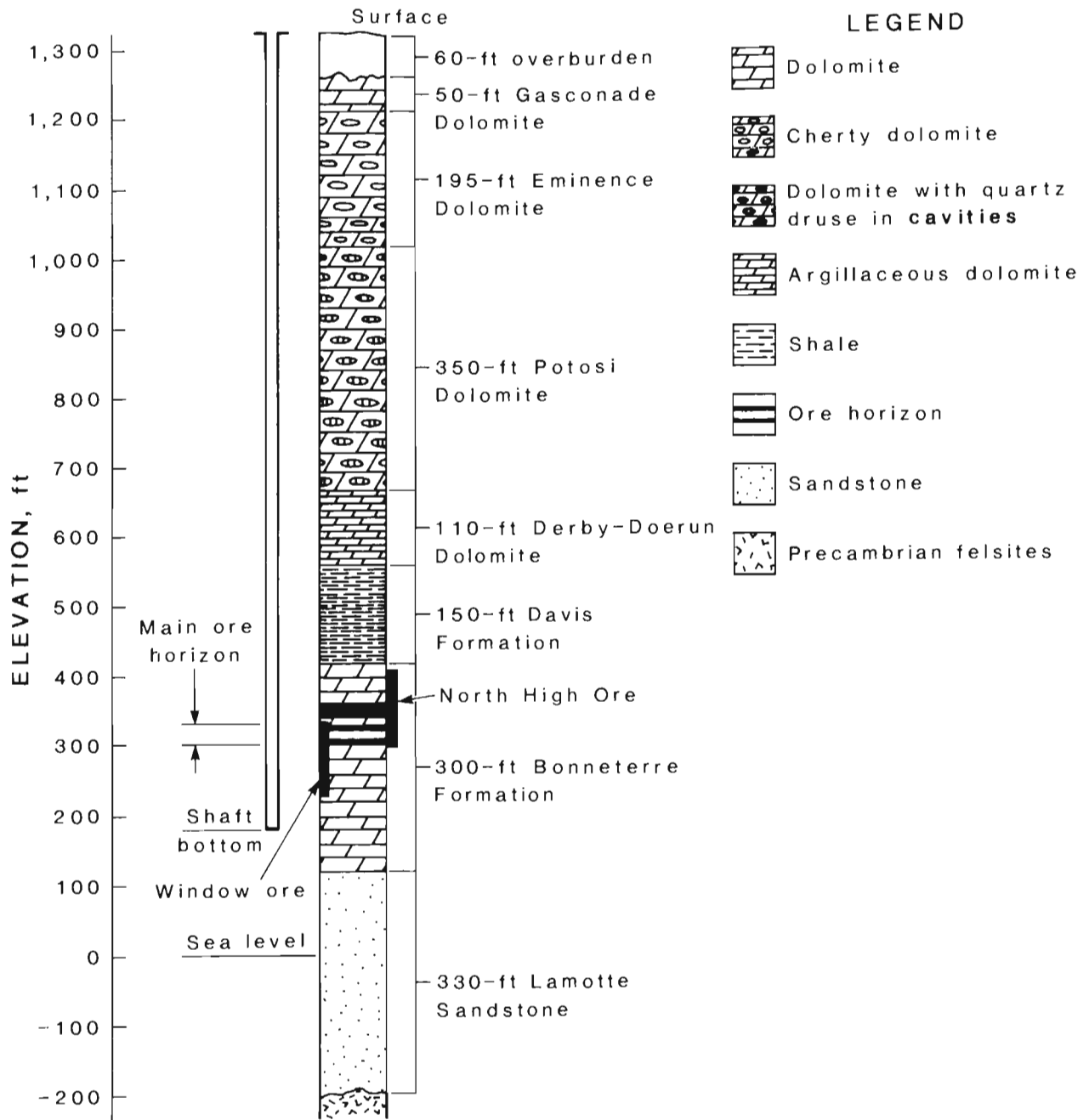Precambrian felsites

Figure 2.—Generalized stratigraphic column of Magmont Mine. After Bradley (2).

PILLAR REMOVAL PROGRAM AND INSTRUMENTATION

In order to maximize ore extraction, the pillars in the North 140 area are being removed sequentially by retreat mining. Pillar 1 was removed first, followed by pillar 2 and 10 ft of its west abutment or rib (fig. 3). Next, pillar 3 was mined along with 10 ft of its west rib. Finally, pillar 4 was removed along with an additional 10 ft of the west rib. Other pillars were and are being removed, but the effect of their removal will not be discussed because the instruments were not functional after pillar 4 was blasted.

Five multiple-point borehole extensometers and two closure extensometers were installed. Extensometers 1 through 3 were installed horizontally in the pillars, and extensometers 4 and 5 were installed vertically in the back. The closure extensometers spanned the distance between the floor and back. Table 1 lists the anchor depths from the hole collar of the borehole extensometers. The purpose of the geotechnical monitoring was to determine the effects of pillar removal on mine stability and to validate a computer model for predicting the effects of further pillar removal.

The borehole extensometers contained linear resistance potentiometers and used hydraulically activated anchors. Stainless steel (1/4-in-diam) rods connected the anchors to the potentiometers. The hole diameters were 2 in for the anchors, 3 in for the collar anchor, and 6 in for the housing unit for the potentiometers. The extensometers were recessed to protect them from flyrock during subsequent removal of pillars. Figure 4 is a schematic of a typical borehole extensometer. The heads of the horizontal extensometers were further protected by mounding tailings beneath the hole collar until the extensometer heads were covered. The cables for extensometers 1, 2, and 4 were buried beneath crosscut 535 to protect them from heavy equipment damage. The cables from the vertical extensometers were encased in airhose and strung along the back and down the side of the pillars. The data acquisition system (DAS) was located in drift 141 at crosscut 534.

The closure extensometers were constructed of telescoping stainless steel tubing connected with cotter pins. Compression in the rods was maintained by a spring inside the tubes. Each unit contained a 6-in linear potentiometer (fig. 5).

Table 1. - Anchor depths and potentiometer lengths for extensometers

Extensometer	Anchor and depth, ft				Potentiometer length, in
	1	2	3	4	
1	15.0	11	6	NAp	6
2	15.0	11	6	NAp	6
3	13.5	11	6	NAp	6
4	41.0	26	11	6	10
5	46.0	26	11	6	10

NAp Not applicable.

Data were collected on cassette tapes controlled by a microcomputer located in the surveyors' room approximately 1,750 ft from the instrumented area. This location provided a relatively clean environment. The computer communicated with the DAS via modems. The computer was initially programmed to take readings every 24 h. The Magmont Mine staff programmed it to record readings every 2 h before and after a pillar was scheduled to be removed.

INSTRUMENT RESPONSE TO MINING

Since the borehole extensometers are considered by the manufacturer to be accurate to 0.001 in and reproducibility is considered to be 0.005 in, any measurement recorded between an anchor and hole collar smaller than 0.001 in was considered to be 0 in. For example, figure 6 A and B show anchors 1 and 2 of extensometer 4 reflecting measurements too small to be significant, and figure 6C shows the effect of the extraction of pillar 2 on the third anchor. In this case, the recorded displacement was approximately 0.00025 in. Although the instrument is not considered to be accurate to this degree, displacement appears to be a direct result of pillar removal. Plots of other instrument readouts also have displacement changes of this amount, but the change cannot always be associated with a blast. The only nonzero displacements attributable to a mining event were recorded by instruments 3 and 7 when pillar 3 was removed. Instrument 3, anchor 3, had a value of -.001 in and instrument 7 had a value of -0.100 in. A negative number indicates that the movement was in a compressive direction.

IN SITU STRESS DETERMINATION

The in situ stress field is one of the most important input parameters to any numeric modeling program. Without it, only an educated guess may be made as to its magnitude and direction. Vertical stress may be calculated on the basis of depth and density of the rock mass, but the influence of horizontal stress requires actual field measurement. There are several instruments and techniques available for performing the in situ stress and related physical property tests. However, for this study, the overcore method of stress determination was selected.

Briefly, this method entails installing some type of strain gauge at depth in a borehole and then drilling past the gauge with a diamond coring bit. The strain gauge measures the expansion of the core as the coring bit relieves pressure. These measurements can then be used to calculate the stress. For this work, the Commonwealth

In situ stress hole

537

536

535

534

533

532

531

138   139   140

531

Cable to computer

Data acquisition
system

141

0   50

Scale, ft

N

LEGEND

1	Pillar number
531	Crosscut number
138	Drift number
⊡	Instrument number
•—	Horizontal borehole extensometer
▪	Vertical borehole extensometer
•	Closure extensometer
▨	Cut 1
◨	Cut 2
▥	Cut 3
▤	Cut 4
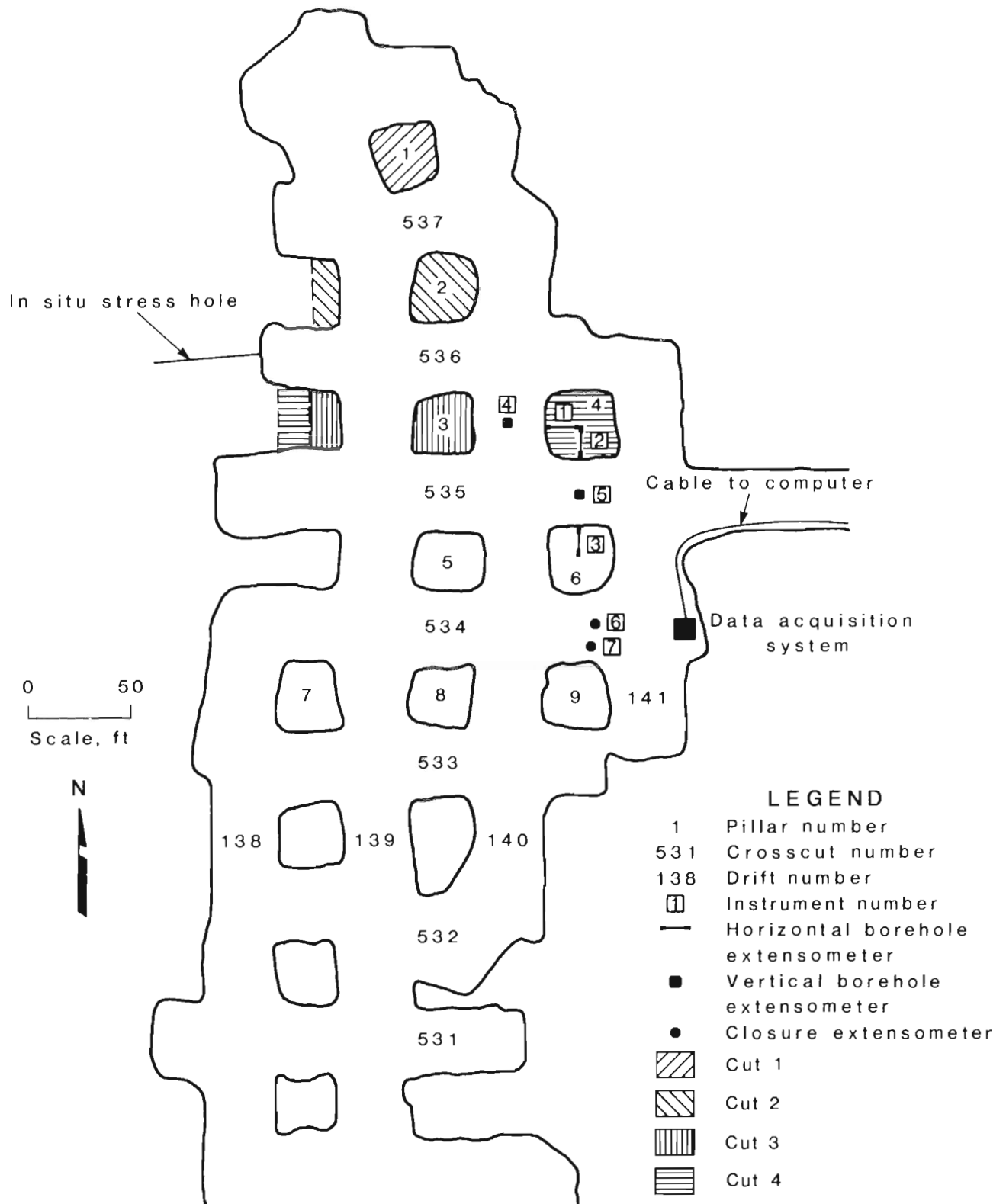
Figure 3.—Plan view of instrumented area.
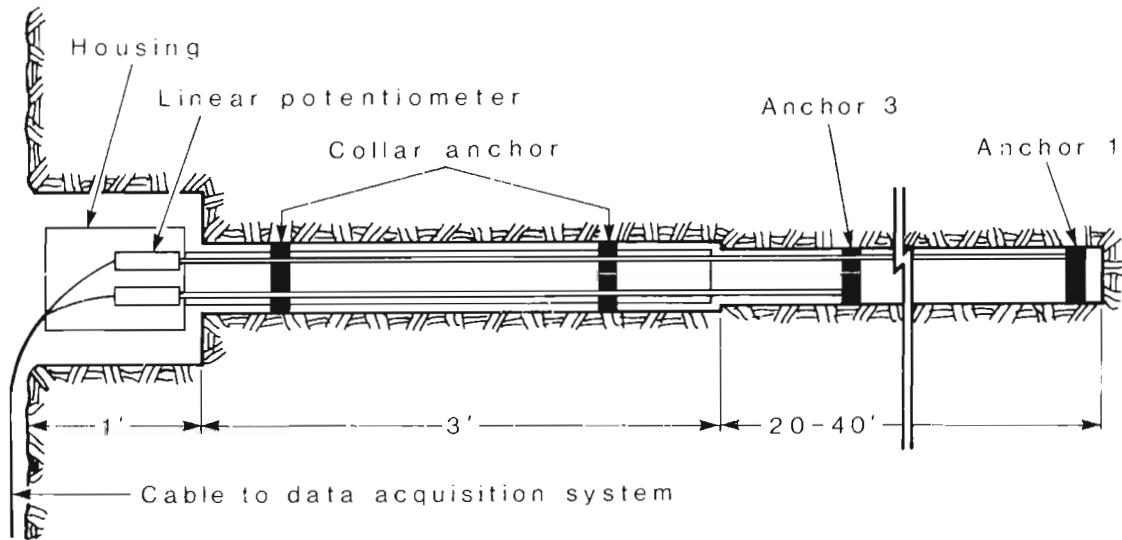
Figure 4.—Typical borehole extensometer (not to scale).
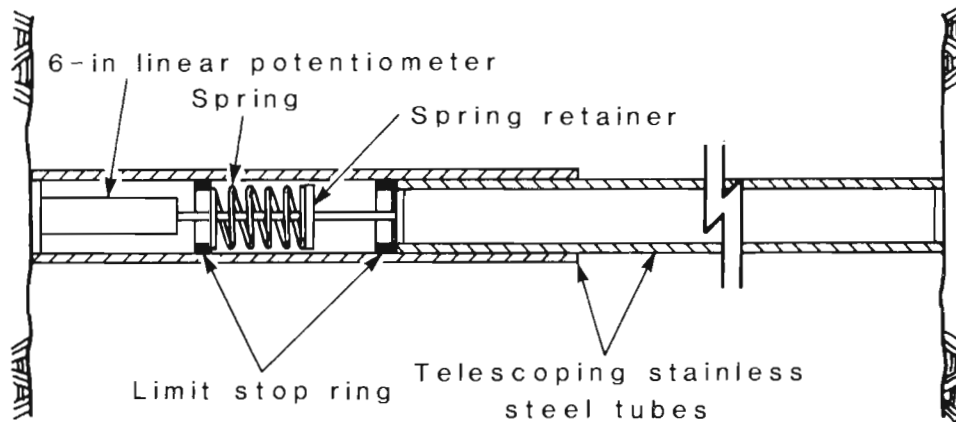
Figure 5.—Schematic of closure extensometer (not to scale).

Scientific and Industrial Research Organization (CSIRO) hollow inclusion cell was used. The CSIRO cell contains nine strain gauges at various orientations. The cell is glued in a 1.5-in-diam pilot hole and then overcored with a 6-in-diam bit. The nine gauges permit measurement of the complete stress field in one borehole as opposed to other methods, which require three holes. Four such cells were installed in a borehole at the west end of the 536 crosscut at depths ranging from 44 to 54 ft (fig. 3). Gauge response was monitored continuously with a DAS during overcoring. Figure 7 shows the DAS connected to the gauge prior to overcoring. The drill is shown on the right.

Principal stresses and stress components are shown in tables 2 and 3. These results indicate that the highest principal stress (in absolute value) is nearly horizontal. Although an attempt was made to take the measurements in an undisturbed area of the mine, there is a possibility that this was not the case and that the measurements were not the true virgin stresses. There is a room-and-pillar area east of the stress measurement location that spans

8

approximately 200 ft and could be considered one large opening. In order to escape the influence of this large opening, it would be necessary to drill over 300 ft. With current techniques, this is not practical.

The possibility that the in situ stress measurements may not be true virgin stresses does not eliminate the ability to use these stresses for input to numerical models. These stresses were used as initial stresses in the two-dimensional, finite-element analyses along with the gravity load.

TABLE 2. - Measured in situ principal stresses

Stress, psi[1]	Dip, deg[2]	Azimuth, deg[3]
-3,557	1.6	239.6
-1,157	85.8	127.7
-499	-3.9	149.7

[1]Minus sign indicates compressive stress.
[2]Dip—angle down from the horizontal (positive).
[3]Azimuth—angle clockwise from north (positive).

TABLE 3. - Measured in situ stress components

(Minus sign indicates compressive stress)

Type of stress	Direction	Amount, psi
Normal	North-south	-1,285
Do	East-west	-2,773
Do	Vertical	-1,156
Shear	North-south, east-west . . .	-1,333
Do	East-west, vertical	34
Do	Vertical, north-south	72
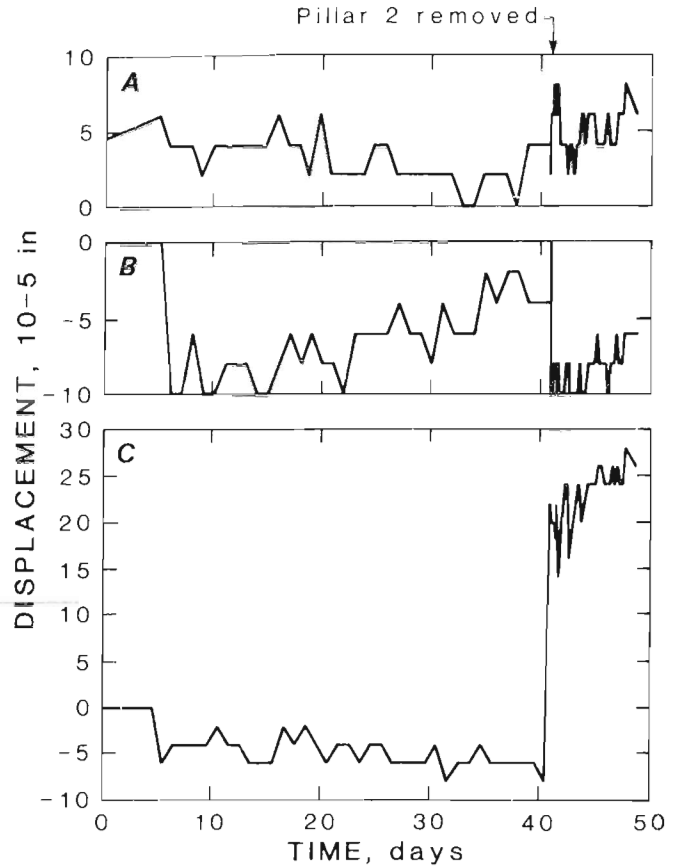
Figure 6.—Displacement versus time, extensometer 4. A, Anchor 1; B, anchor 2; C, anchor 3.
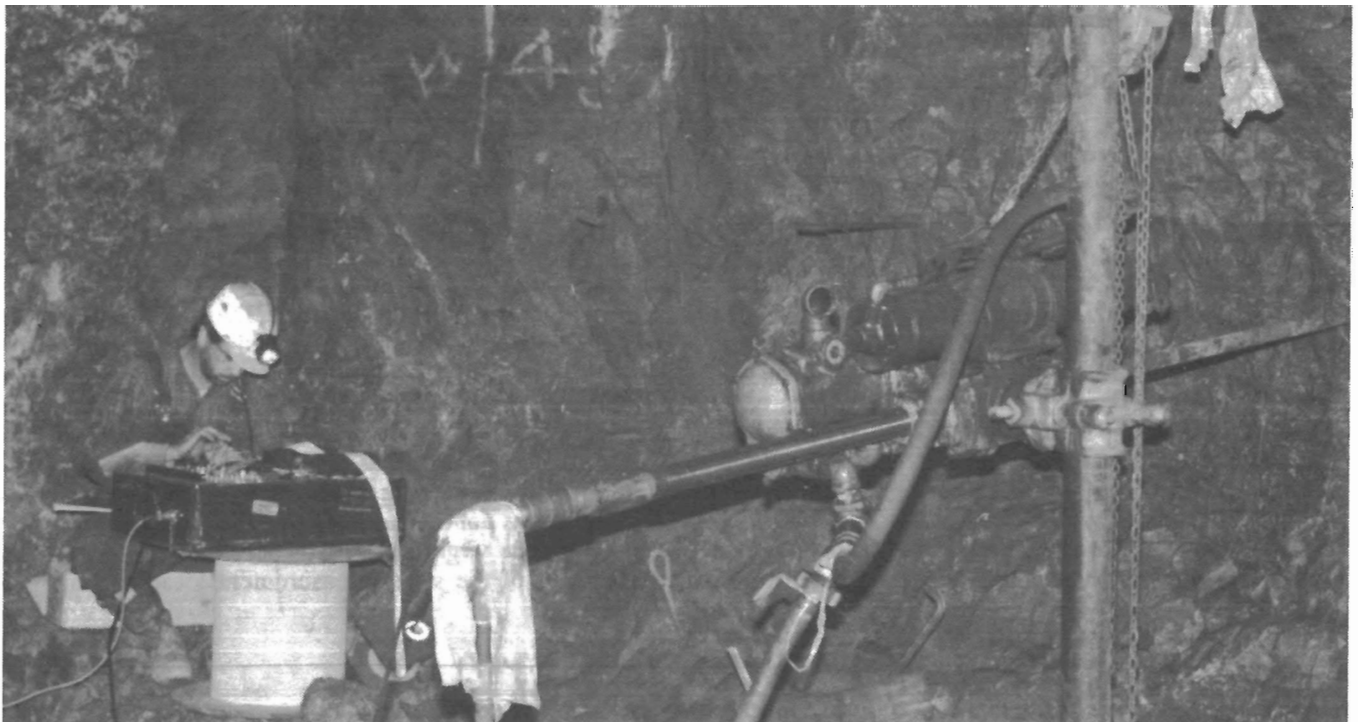
Figure 7.—DAS connected to gauge prior to overcoring.

MATERIAL PROPERTY DETERMINATION

In order to determine whether the host rock exhibited any anisotropic behavior, physical properties were obtained for three orthogonal directions by redrilling some of the 5.62-in-diam in situ stress cores. After setting this larger core in a fixture (fig. 8), smaller (1.77-in-diam by about 4 in long) cores were obtained using a thin-walled masonry bit. These small cores were oriented along the big core axis as well as perpendicular to its axis in two planes 90° apart. Since the orientation of the large core was known, the fixture was adjusted to provide small cores in the one vertical and two horizontal axes. Figure 9 shows the size of the small cores in relation to the in situ stress cores.

Unconfined compression tests were performed on the smaller cores to determine the elastic modulus, Poisson's ratio, and unconfined compressive strength (table 4). Each sample was weighed and density was calculated. Based on these limited data, it was decided that the host rock would be considered isotropic for modeling purposes. Tensile strength was determined from other core samples of the host rock using the Brazilian tensile test.[5] Table 5 lists the results of these tests.

---

[5]Test procedures are described by the American Society for Testing and Materials, standard test method no. D 3967-86. The core samples were approximately 2.686 in diam and 1.456 in long.

Figure 8.—Setting 6-in core in fixture.

TABLE 4. - Density, elastic modulus, Poisson's ratio, and unconfined compressive strength of host rock

Test	Density, pcf	Elastic modulus, psi × 10^6	Poisson's ratio	Strength,[1] psi	Test	Density, pcf	Elastic modulus, psi × 10^6	Poisson's ratio	Strength,[1] psi
Vertical:					Horizontal:[3]				
1	173.6	13.83	0.25	-25,500	6	171.9	11.67	.33	-19,286
2	169.8	14.00	ND	-18,500	7	170.8	14.03	.29	-20,938
3	171.3	13.50	.29	-18,000	8	168.0	12.33	.31	-28,862
4	171.7	ND	ND	-16,622	9	170.8	7.30	.22	-20,485
5	172.9	14.00	.27	-17,625	10	172.7	14.62	ND	-14,907
Average	171.9	13.83	.27	-19,249	Average	170.8	11.99	.26	-20,896
Horizontal:[2]					Overall av ..	171.5	13.41	.26	-21,278
1	171.2	12.74	.26	-17,667					
2	172.4	7.90	.26	-22,024					
3	172.1	27.08	.12	-21,250					
4	171.9	13.20	ND	-33,830					
5	170.9	11.10	.26	-23,678					
Average	171.7	14.40	.23	-23,690					

ND No data.
[1]Unconfined compressive strength.
[2]Cores drilled horizontal and perpendicular to borehole axis.
[3]Cores drilled horizontal and in same direction as borehole axis.

TABLE 5. - Laboratory tensile strengths for the host rock

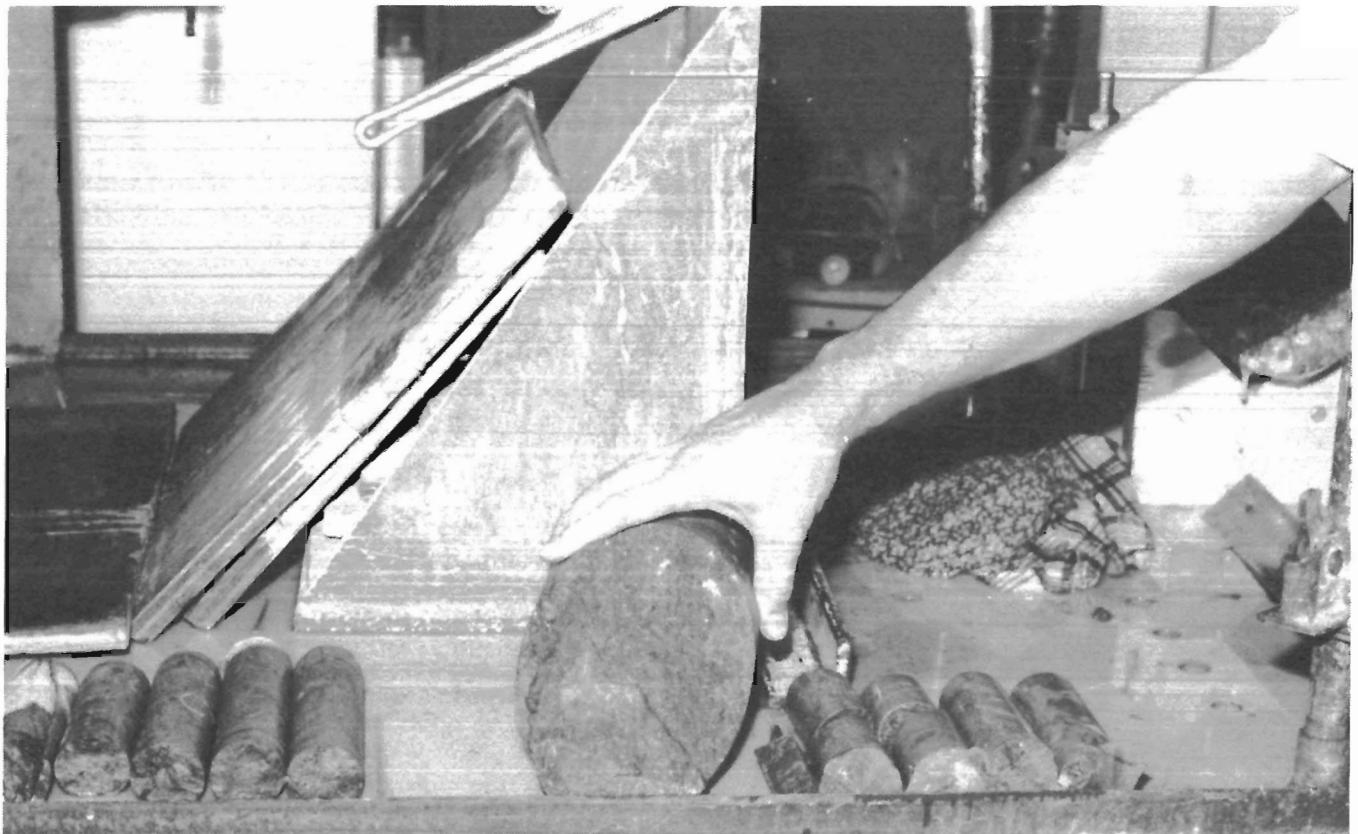| Density, pcf	Tensile strength, psi	Density, pcf	Tensile strength, psi
176	1,770	178	356
176	939	179	1,543
176	1,502	183	1,488

Figure 9.—Oriented 1.77-in cores obtained from 6-in overcore.

NUMERICAL MODELS

Three numerical models were used to analyze the pillar recovery program: the two-dimensional, finite-element program UTAH2; the three-dimensional, finite-element program UTAH3; and the three-dimensional, displacement discontinuity program THREED. Two loading cases were used for each model: gravity load and in situ load. The in situ load case was based on in situ measurements obtained in the west rib of the North 140 area.

The factor of safety, a ratio of rock strength to stress, was used along with principal stresses to compare the results from the different loading conditions and models. A factor of safety near unity would mean that the pillar is close to failure.

TWO-DIMENSIONAL, FINITE-ELEMENT MODEL

The two-dimensional, finite-element program used to model cross sections of the Magmont North 140 was UTAH2 (3). This program can be used for strictly elastic or elastic-plastic analyses in plane strain or plane stress. The yield criterion is Drucker-Prager where strength is dependent on all three principal stresses and the associate flow rules are applied for determining strains in yielded elements.

Two cross sections of the North 140 were modeled in plane strain: an east-west cross section through pillars 3 and 4 and a north-south cross section through pillars 4, 6, and 9. The finite element mesh had 2,194 elements and 2,178 nodes. The mesh was divided into 5- by 5-ft elements near the excavations and 50- by 50-ft elements in most other areas. The entire mesh was 1,695 ft vertically and 1,800 ft horizontally. The top of the mesh represented the ground surface, so gravity load was applied through the weight of the material. The material layers from the top of the mesh included 60 ft of overburden at 130 pcf, 705 ft of dolomite at 172 pcf, 150 ft of shale at 137 pcf, and 780 ft of dolomite at 172 pcf. The specific weight of the dolomite was the average value from the laboratory specimens. Other specific weights were averages of reported values (4). Average reported laboratory test values were also used for the density, elastic modulus, Poisson's ratio, and unconfined compressive strength of the shale and overburden. Isotropic media were assumed.

Two initial stress cases were run for each cross section. In the first case, only gravity load was applied to the mesh. Any initial horizontal stresses were due to the Poisson effect. In the second case, horizontal stresses were applied such that the horizontal stresses due to the Poisson effect (gravity), when added to additional horizontal stresses, yielded the in situ stress measurement. The horizontal stress distribution was assumed to increase linearly with depth starting with a value of 0 at the surface. The in situ vertical stress was measured as -1,156 psi, which is close to the stress caused by the weight of the material; therefore, extra stress was not added in the vertical direction.

Since the mesh consisted of a 150-ft-thick layer of shale above the ore zone, the assumed stress distribution created an incompatible strain state at the boundary between the shale and dolomite because of the different elastic moduli. To determine if this would have a significant effect on the stress state around mine openings, a comparative computer run was made using the initial stresses calculated from a triangular strain distribution. Both runs yielded the same results around the mine openings.

The mining sequence for the east-west cross section consisted of cutting drifts 139 and 140, filling the drifts with 7 ft of tailings, removing pillar 3 along with 10 ft of the west abutment, and finally removing pillar 4 with 10 additional ft of the west abutment.

The mining sequence for the north-south cross section consisted of excavating crosscuts 533 through 536, filling the crosscuts with 7 ft of tailings, and excavating pillar 4. At this point in the mining sequence, the extensometers were either destroyed when the pillar was removed or not functioning.

Principal stress and factor-of-safety contours from the two-dimensional, finite-element analyses are shown in figures A-1 through A-30 in the appendix.

TWO-DIMENSIONAL, FINITE-ELEMENT RESULTS, GRAVITY LOAD CASE

Figures A-2, A-5, and A-8 show the contours of the minor principal stresses (greatest compression) of the east-west cross section as mining progressed. Compressive stress concentrations occurred at the corners of the openings. The highest stress after excavation of the entries was -2,700 psi in pillar 3. The removal of pillar 3 along with 10 ft of the west abutment caused redistribution of stresses into pillar 4 and the west abutment. Maximum compressive values for the minor principal stresses in both these areas were -4,000 psi. This is an additional -1,900 psi in the west abutment and -1,500 psi in pillar 4. The factor of safety in pillar 4 was reduced by approximately 1.0 by the removal of pillar 3.

The removal of pillar 4 increased the maximum compressive stress in the west abutment from -4,000 to -5,100 psi and increased the maximum compressive stress in the east abutment from -2,600 to -4,900 psi. The factor-of-safety contour line in the abutment areas had a value of 4. Tensile stresses in elements in the back above entry 140 exceeded 800 psi. Combined stresses yielded a factor of safety of 3 in this area.

The minor principal stresses in the north-south cross section are shown in figures A-11 and A-14. Maximum compressive stresses of -2,900 psi occurred in pillars 4 and 6 and in the rib area of crosscut 535. Maximum compressive stresses of -2,700 and -2,500 psi occurred in pillars 6 and 9, respectively. The removal of pillar 4 and the brow above crosscut 535 increased the maximum compressive

stress in pillar 6 to -4,000 psi and the maximum compressive stress in pillar 9 to -3,200 psi. In terms of factors of safety, the values were reduced from a minimum of 5 to a minimum of 4 in both pillars (figs. A-12, A-15). The minimum factor of safety above the new span is now 8.

Predicted relative displacements between the anchors and collar of the borehole extensometers ranged from -0.0037 to 0.0030 in. The range for the closure extensometers was -0.0219 in to -0.0173 in.

TWO-DIMENSIONAL, FINITE-ELEMENT RESULTS, IN SITU LOAD CASE

For the east-west cross section after the removal of the entries and crosscuts, the minor principal stresses (greatest compression) in the pillars were within 200 psi of the gravity load case (figs. A-2, A-17). The stresses above the entries, however, differed as much as 3,200 psi, where the greater compressive stress occurred in the in situ stress case. The stresses in the abutments were also higher for this case. The factors of safety in the back and abutments were lower (figs. A-3, A-18). When pillar 4 was extracted, the factors of safety in the back were approximately equal to 4 for both cases (figs. A-9, A-24). The values remained in this range for about 90 ft above the opening for the in situ stress case, but rapidly increased for the gravity load case.

The principal stress and factor-of-safety contours of the north-south cross section are shown in figures A-25 through A-30. The largest compressive stresses before the removal of pillar 4 were in pillars 4 and 6 with values up to -2,900 psi. This was similar to the gravity load case. However, the stresses in the back above the crosscuts were up to -1,000 psi more. This was reflected in the reduction in the factor of safety in the back. These values were up to one-fifth the factor-of-safety values for the case without the in situ load present. The factors of safety in the pillars were approximately the same for both cases.

The results were similar when pillar 4 was removed. Maximum compressive stresses increased in pillar 6 from -2,700 to -4,000 psi and in pillar 9 from -2,500 to -3,000 psi for both loading conditions. The factors of safety in the pillars and abutments were the same with a minimum of 4 in pillar 4 and the north rib of crosscut 536. The factor of safety above crosscut 533 for the in situ stress case was 6. This is one-tenth the value obtained from the gravity load case.

Predicted relative displacements between the anchors and collar of the borehole extensometers ranged from -0.0030 in to 0.0053 in. The range for the closure extensometers was -0.0228 to -0.0183.

THREE-DIMENSIONAL, FINITE-ELEMENT RESULTS, GRAVITY LOAD CASE

The three-dimensional, finite-element program UTAH3 was used to model the North 140 area with gravity loading. The same stratigraphy as in the two-dimensional case was used. The pillar dimensions and locations were altered slightly in order to use an automatic mesh generator. Each pillar was 30 by 30 ft in plan view and 25 ft in height. The mesh was very coarse, but still consisted of 11,040 elements and 12,648 nodes; each pillar was represented by one element. Although the mesh was coarse, it provided an estimate of average pillar stresses and factors of safety. A refined mesh in the areas of the extensometers would be necessary to compare the three-dimensional results with the two-dimensional results and the measured data.

Table 6 lists average vertical and horizontal pillar stresses before the pillar recovery program began and after each pillar was removed. Table 7 lists the pillar factors of safety based on average pillar stresses, which ranged from 3.9 to 4.7, and illustrates that the removal of pillars 1 through 4 did not have a significant impact on pillar factors of safety. Table 8 shows that pillar factors of safety were reduced by a maximum of 1.0 when only vertical stresses were used in the calculation.

Factors of safety in pillars 3 and 4 calculated by UTAH2 were larger than those calculated by UTAH3. After the entries and crosscuts were mined, the pillar factors of safety predicted by UTAH2 ranged from 5 to 6 while UTAH3 predicted a factor of safety of 4.3 for pillar 3 and 4.5 for pillar 4. However, when pillar 3 was removed, the safety factor in pillar 4 predicted by UTAH2 was between 4 and 5, while that predicted by UTAH3 was 4.5.

Similarly, factors of safety for pillars 4, 6, and 9 as predicted by UTAH2 were higher than those predicted by UTAH3 after the entries and crosscuts were removed. When pillar 4 was removed, the average factor of safety in pillar 6 was the same for both codes (a value of 4.0), but in pillar 9, it was higher for the two-dimensional case. These results indicate that additional overburden load should be applied when using the two-dimensional code to account for the crosscuts or entries not in the plane of the analysis. The use of a method based on average pillar stresses, tributary loading, and the extraction ratio (5) is a possibility; however, this method may not be applicable because the North 140 is not an extensive room-and-pillar area. The abutments may be too close to the pillars to use this method effectively.

THREE-DIMENSIONAL, FINITE-ELEMENT RESULTS, IN SITU LOAD CASE

Initial stress gradients were produced such that when they were added to the gravity stress state, the in situ stress state at the measurement location was achieved. The stresses were assumed to vanish at the surface.

As in the three-dimensional gravity load case, the effect of the removal of the pillars was not significant on the factor of safety of the pillars. The overall values, however, were higher by approximately 1.0 for the in situ load case (table 9). This was not the case in two dimensions where the pillar factor of safety remained the same.

TABLE 6. - Average pillar stresses predicted by three-dimensional, finite-element model with gravity load, pounds per square inch

(Minus sign indicates compressive stress)

Area mined	Pillar number								
	1	2	3	4	5	6	7	8	9
	VERTICAL STRESSES								
Entries, crosscuts	-3,472	-3,609	-3,752	-3,578	-3,785	-3,667	-3,296	-3,571	-3,293
Pillar 1	NAp	-3,957	-3,801	-3,609	-3,795	-3,674	-3,298	-3,573	-3,295
Pillar 2	NAp	NAp	-4,203	-3,781	-3,851	-3,714	-3,306	-3,584	-3,303
Pillar 3	NAp	NAp	NAp	-4,337	-4,276	-3,905	-3,344	-3,643	-3,345
Pillar 4	NAp	NAp	NAp	NAp	-4,551	-4,383	-3,369	-3,699	-3,411
	HORIZONTAL STRESSES								
Entries, crosscuts	-926	-962	-1,000	-962	-1,011	-984	-900	-961	-897
Pillar 1	NAp	-1,050	-1,014	-975	-1,016	-988	-902	-963	-899
Pillar 2	NAp	NAp	-1,118	-1,023	-1,036	-1,004	-906	-969	-905
Pillar 3	NAp	NAp	NAp	-1,159	-1,142	-1,058	-921	-990	-921
Pillar 4	NAp	NAp	NAp	NAp	-1,213	-1,178	-932	-1,010	-945

NAp Not applicable.

TABLE 7. - Pillar factors of safety predicted by three-dimensional, finite-element model with gravity load, based on average pillar stresses

Area mined	Pillar number								
	1	2	3	4	5	6	7	8	9
Entries, crosscuts . .	4.5	4.4	4.3	4.5	4.3	4.4	4.7	4.7	4.7
Pillar 1	NAp	4.2	4.3	4.5	4.3	4.4	4.7	4.5	4.7
Pillar 2	NAp	NAp	4.0	4.3	4.3	4.4	4.7	4.5	4.7
Pillar 3	NAp	NAp	NAp	4.0	4.0	4.3	4.7	4.5	4.7
Pillar 4	NAp	NAp	NAp	NAp	3.9	4.0	4.7	4.4	4.7

NAp Not applicable.

TABLE 8. - Pillar factors of safety predicted by three-dimensional, finite-element model with gravity load, based on average vertical stresses

Area mined	Pillar number								
	1	2	3	4	5	6	7	8	9
Entries, crosscuts . .	6.1	5.9	5.7	5.9	5.6	5.8	6.5	6.0	6.5
Pillar 1	NAp	5.4	5.6	5.9	5.6	5.8	6.5	6.0	6.5
Pillar 2	NAp	NAp	5.1	5.6	5.5	5.7	6.4	5.9	6.4
Pillar 3	NAp	NAp	NAp	4.9	5.0	5.4	6.4	5.8	6.4
Pillar 4	NAp	NAp	NAp	NAp	4.7	4.9	6.3	5.8	6.2

NAp Not applicable.

TABLE 9. - Pillar factors of safety predicted by three-dimensional, finite-element model with in situ load

Area mined	Pillar number								
	1	2	3	4	5	6	7	8	9
Entries, crosscuts . .	5.3	5.5	5.4	5.5	5.4	5.4	5.4	5.5	5.6
Pillar 1	NAp	5.4	5.4	5.5	5.4	5.4	5.4	5.5	5.6
Pillar 2	NAp	NAp	5.4	5.4	5.5	5.4	5.5	5.5	5.6
Pillar 3	NAp	NAp	NAp	5.2	5.4	5.4	5.5	5.5	5.6
Pillar 4	NAp	NAp	NAp	NAp	5.4	5.3	5.5	5.6	5.6

NAp Not applicable.

TABLE 10. - Element factors of safety in the back above pillars 3 and 4 predicted by three-dimensional, finite-element model

Area mined	Gravity load			In situ load		
	Above pillar 3	Between pillars 3-4	Above pillar 4	Above pillar 3	Between pillars 3-4	Above pillar 4
Entries, crosscuts . .	9.3	10.7	9.8	4.0	3.6	4.0
Pillar 1	9.2	10.7	9.7	4.0	3.7	4.0
Pillar 2	8.4	10.0	9.4	4.0	3.7	4.1
Pillar 3	18.3	8.2	8.4	3.3	8.5	4.1
Pillar 4	17.0	17.9	20.7	3.3	3.2	3.3

The factor of safety in the back differed greatly for in situ loading versus gravity loading as they did in the two-dimensional case (table 10). The values for the in situ loading case are up to one-sixth the values of the gravity load case.

DISPLACEMENT DISCONTINUITY CODE

The extraction of the pillars in the North 140 area was also modeled in plan view using the displacement discontinuity code THREED (6). In solving this problem, it was assumed that the seam to be excavated lay at infinite depth. In practice, this is not the case, but it has been shown that in two dimensions, the stresses and displacements induced by a single slitlike excavation are relatively unaffected by the surface if the width of the excavation is less than the depth of overburden. Other assumptions were that the seam lay in a principal plane, the thickness of the seam was small relative to the entire rock mass, and the displacements at the boundaries were zero.

The input and output for the program referred to a 120- by 120-unit grid resulting in 14,400 squares. The outer 5 squares were used as a fixed boundary, leaving a 110- by 110-unit grid for the computations. For the Magmont North 140 area, each square represented 10 ft. The rock surrounding the seam was modeled in the elastic mode. The same elastic modulus and Poisson's ratio were used as those used in the finite-element runs. The seam can be modeled strictly elastically or in a strain-softening mode where the stress-strain curve is represented by line

TABLE 11. - Average vertical pillar stresses predicted by displacement discontinuity model, pounds per square inch

(Minus sign indicates compressive stress)

Area mined	Pillar number								
	1	2	3	4	5	6	7	8	9
	VERTICAL STRESSES								
Entries, crosscuts	-2,956	-2,876	-4,173	-3,325	-3,941	-3,607	-3,488	-3,800	-3,084
Pillar 1 mined	NAp	-3,432	-4,173	-3,325	-3,941	-3,607	-3,488	-3,800	-3,084
Pillar 2 mined	NAp	NAp	-4,527	-3,489	-4,015	-3,669	-3,547	-3,800	-3,084
Pillar 3 mined	NAp	NAp	NAp	-3,669	-4,172	-3,733	-3,547	-3,800	-3,084
Pillar 4 mined	NAp	NAp	NAp	NAp	-4,433	-4,015	-3,607	-3,941	-3,176

NAp Not applicable.

segments. Up to three stress-strain curves can be entered for the seam material. In this manner, stronger material can be accounted for as the distance from the face increases. The load modulus, however, must be the same in all cases. Strictly elastic material was assumed for modeling the Magmont North 140.

Pillars 1 through 4 were removed sequentially in the model. Vertical pillar stresses are shown in table 11, and pillar factors of safety based on these stresses are listed in table 12. The version of THREED used limited the size

TABLE 12. - Pillar factors of safety using vertical stresses predicted by displacement discontinuity code

Area mined	Pillar number								
	1	2	3	4	5	6	7	8	9
Entries, crosscuts ..	7.2	7.4	5.1	6.4	5.4	5.9	6.1	5.6	6.9
Pillar 1	NAp	6.2	5.1	6.4	5.4	5.9	6.1	5.6	6.9
Pillar 2	NAp	NAp	4.7	5.8	5.1	5.7	6.0	5.6	6.9
Pillar 3	NAp	NAp	NAp	5.8	5.1	5.7	6.0	5.6	6.9
Pillar 4	NAp	NAp	NAp	NAp	4.8	5.3	5.9	5.4	6.7

NAp Not applicable.

of the grid squares to 10 by 10 ft, which meant that some pillars did not exactly match the dimensions of the instrumented pillars.

COMPARISON OF MEASURED AND PREDICTED DISPLACEMENTS

Because of the limited number of instruments, their low survival rate in the mine environment, and the order of magnitude of movement for most of the instruments, a regression line of predicted versus measured displacements was not possible. Since pillars 1 and 2 were removed simultaneously with pillar 3 in the two-dimensional analysis, a comparison of predicted versus measured displacements for the extraction of these two pillars could not be made. This situation also applied to the removal of pillar 3 when the north-south cross section was modeled. A three-dimensional analysis with a finely graded mesh at the extensometer locations would help rectify this problem.

CONCLUSIONS

The North 140 section of Cominco American's Magmont Mine was monitored with borehole and closure extensometers during pillar removal operations. The mining sequence was modeled using a two-dimensional, finite-element code; a three-dimensional, finite-element code; and a displacement discontinuity code. Gravity loading and in situ load conditions were used in the finite-element runs.

In situ stress measurements were taken in the west rib of the area. It was found that the highest principal stress was nearly horizontal and exceeded the vertical stress. Core samples from the in situ stress measurements were used to obtain smaller oriented samples for laboratory testing.

One purpose of the monitoring program was to validate computer models to use in predicting the effects of additional pillar removal. This was to be accomplished by comparing predicted and measured displacement values and adjusting the elastic moduli in the computer programs accordingly. Because of the limited number of instruments, the loss of some of them during blasting, and the fact that most of the displacement was less than 0.001 in, there were not enough data to validate any of the models for predictive purposes. However, some general observations concerning the global stability of the area and the differences between the results of the computer models can be made.

Both instrument response and predictive models indicated that there was very little or no movement in the area when the pillars involved in this study were removed. Only two instruments showed measurable responses during pillar extraction. Predicted displacements at the instrument locations from the two-dimensional model ranged from -0.0228 to +0.0053 in.

There were no indications of instability during removal of the pillars involved in this study. As predicted by the computer codes, open spans up to 205 ft were achieved with a factor of safety no lower than 3.

The presence of horizontal in situ stresses in the two-dimensional computer model did not have an impact on calculated pillar stability, but reduced the calculated factor of safety in the back by a factor of 10. In situ stresses in the three-dimensional model caused an increase in the calculated pillar factor of safety by approximately 1.0, but the factors of safety in the back were reduced to over one-sixth the values for the gravity load case at some locations.

The mining of pillars 1 through 4 as modeled in this study did not have significant impact on pillar stability as indicated by the calculated factor of safety. The greatest difference in the calculated factor of safety before and after all four pillars were removed during mining was 0.4 for the three-dimensional models and approximately 1.0 for the two-dimensional models.

In general, the three-dimensional code predicted equal or higher compressive stress values and lower factors of safety than the two-dimensional analysis. More work is necessary to determine what effect element gradation has on stress prediction using the three-dimensional code. Advances in three-dimensional, finite element technology as applied to rock mechanics would facilitate such a study.

REFERENCES

1. Magmont Mine Staff. Magmont Operation In-house pamphlet. Bixby, MO. Jan. 1982, 4 pp.

2. Bradley, M. Geology—North High Ore and Window Properties. Magmont Mine, In-house rep., Oct. 1984, 16 pp.

3. Pariseau, W. G. Interpretation of Rock Mechanics Data (contract HO220077, Dep. of Min. Eng., Univ. of UT). v. 2, 1978, 41 pp.

4. Farmer, I. W. Engineering Properties of Rocks. E. and F. N. Spon, Ltd., 1968, 180 pp.

5. Pariseau, W. G. Inexpensive But Technically Sound Mine Pillar Design Analysis. Int. J. Numeri. and Anal. Methods in Geomech., v. 5, 1981, pp. 429-447.

6. Crouch, S. L., and C. Fairhurst. The Mechanics of Coal Mine Bumps and the Interaction Between Coal Pillars, Mine Roof, and Floor (contract HO101778, Dep. Civ. and Miner. Eng., Univ. MN). BuMines OFR 53-73, 1973, 88 pp.; NTIS PB 222-898.

APPENDIX.–PRINCIPAL STRESS AND FACTOR OF SAFETY CONTOURS

Principal stress and factor-of-safety contours from the two-dimensional, finite-element analysis are shown in figures A-1 through A-30. Stress values are in pounds per square inch.
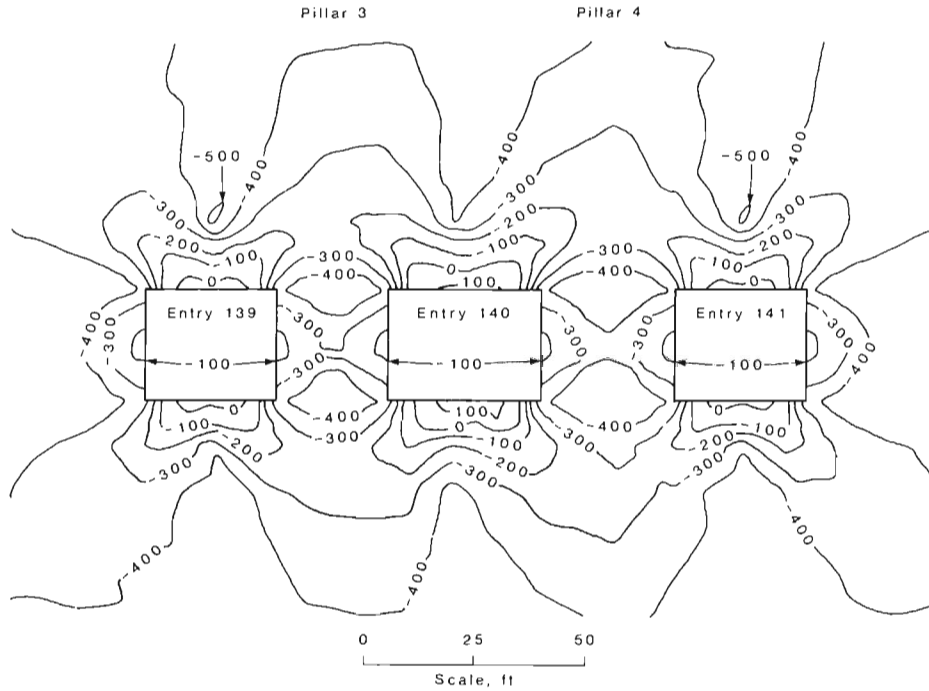
Figure A–1.–East-west cross section of major principal stress contours with entries removed, gravity load case.
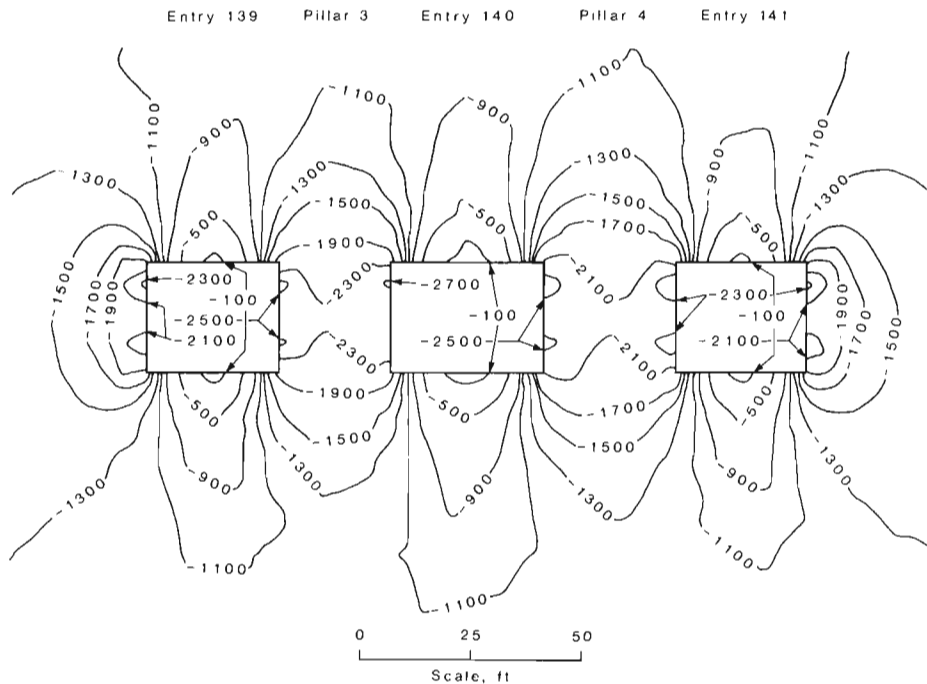
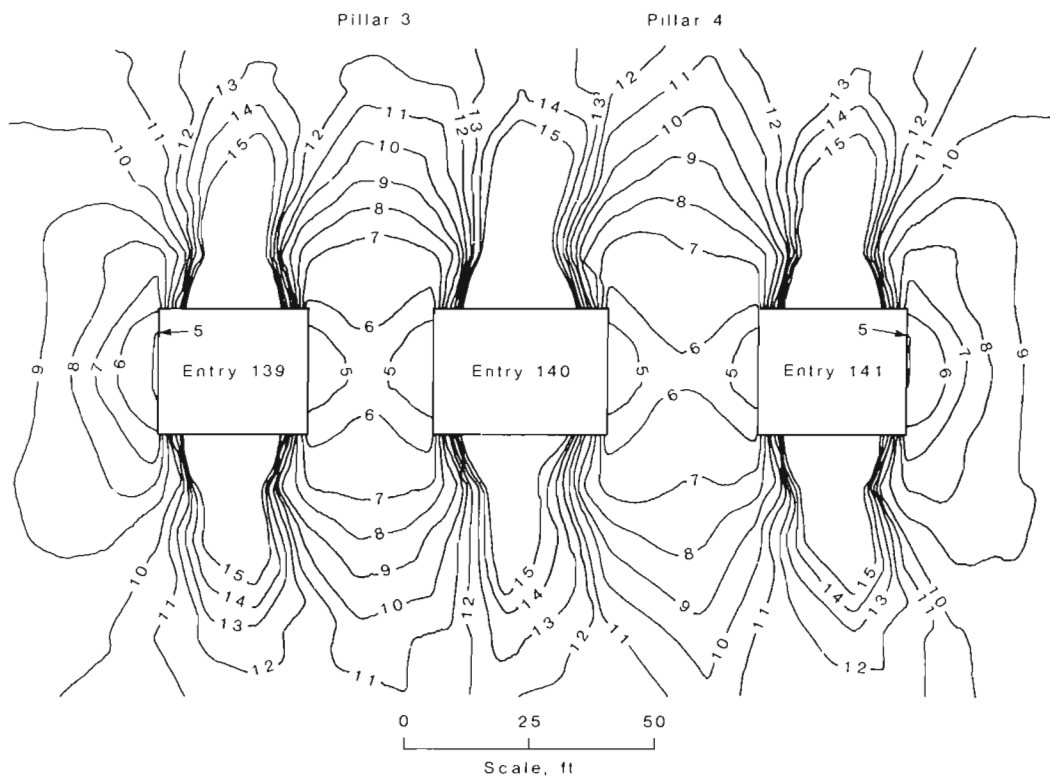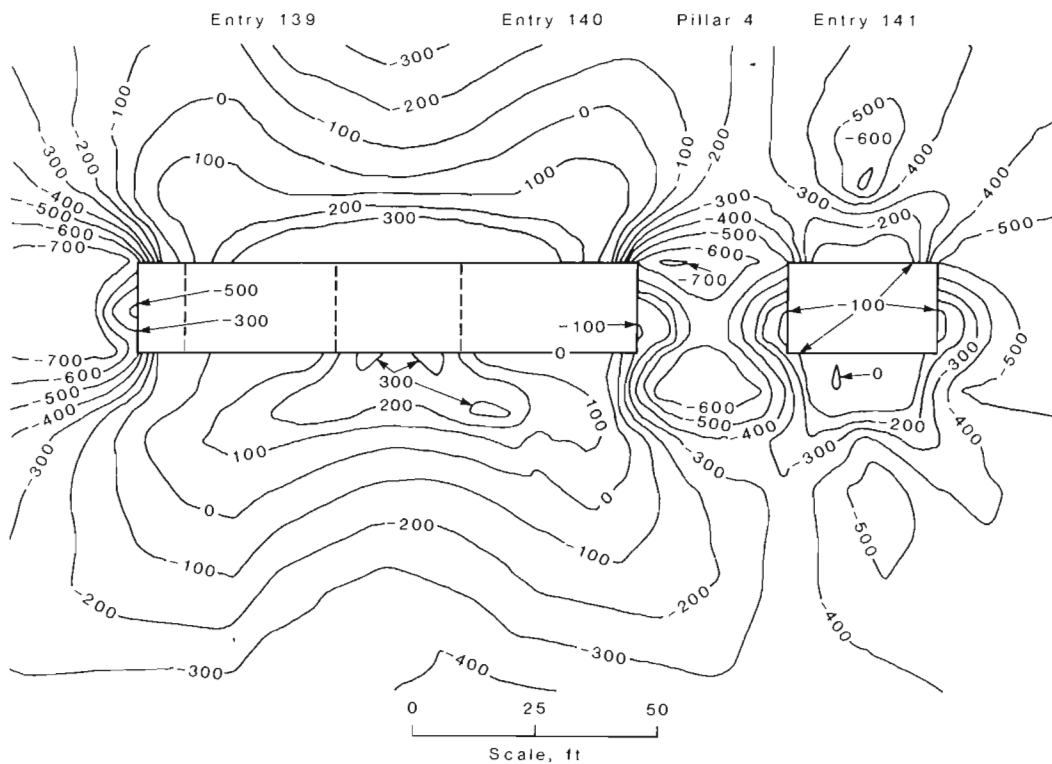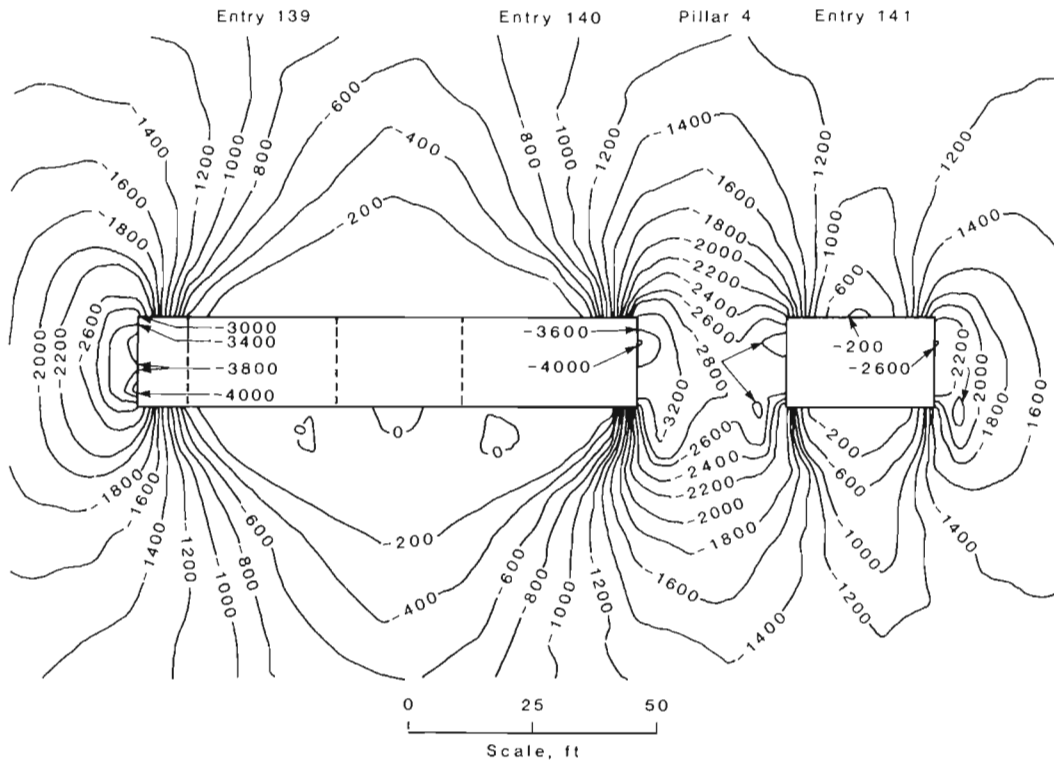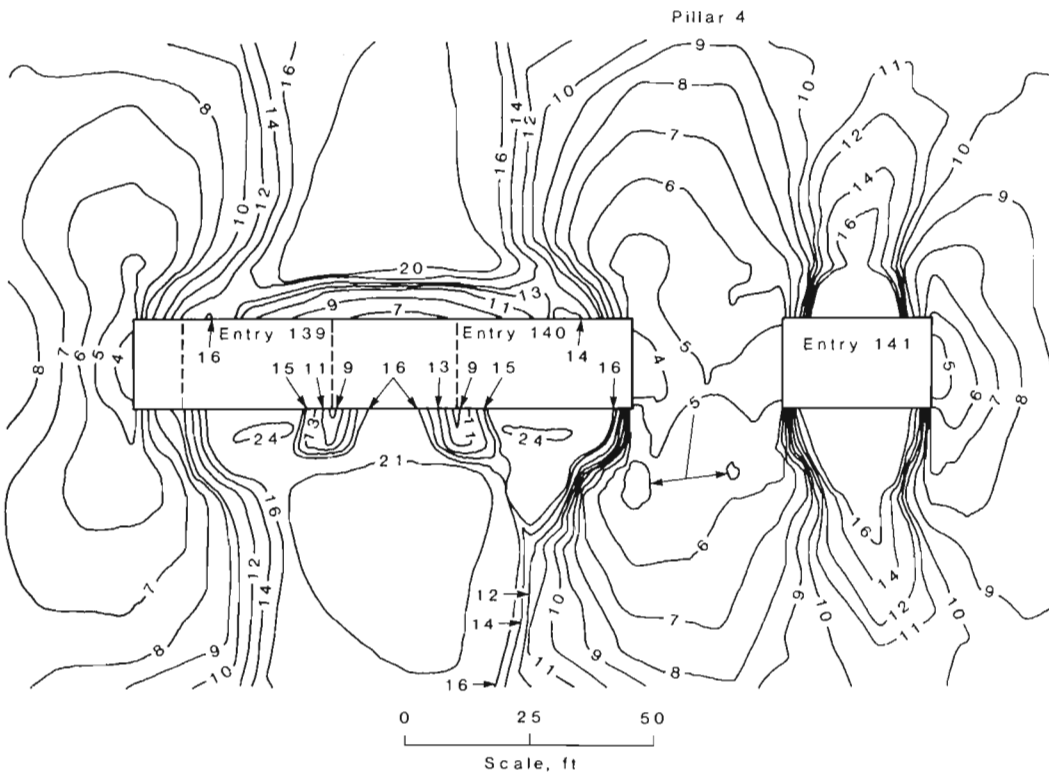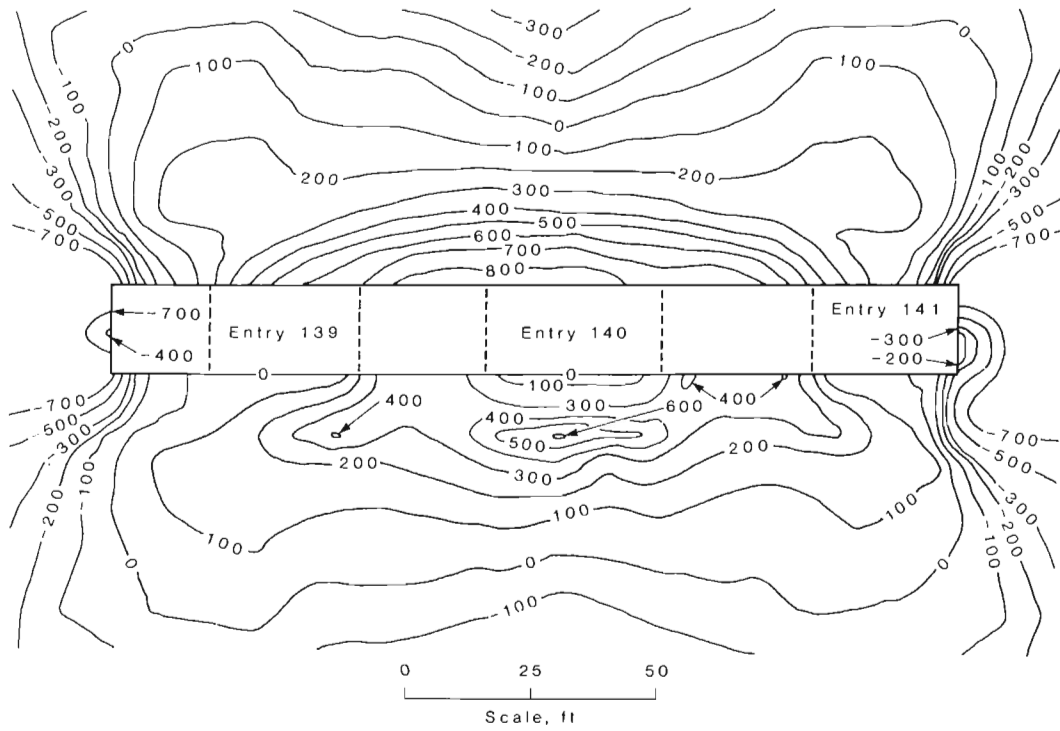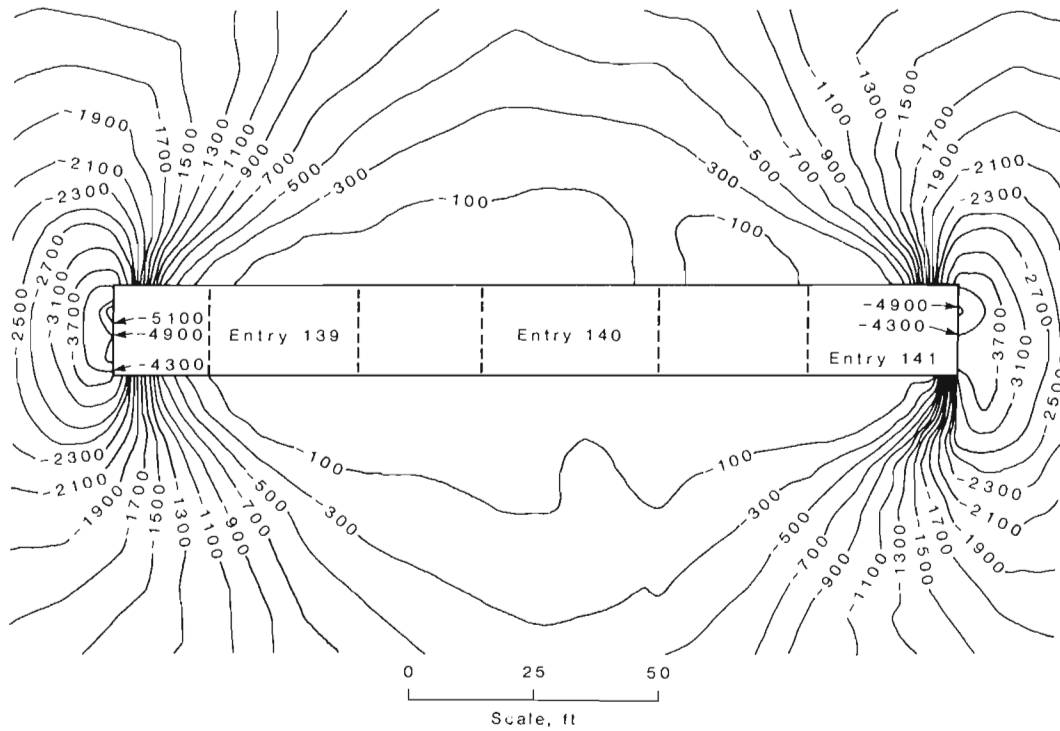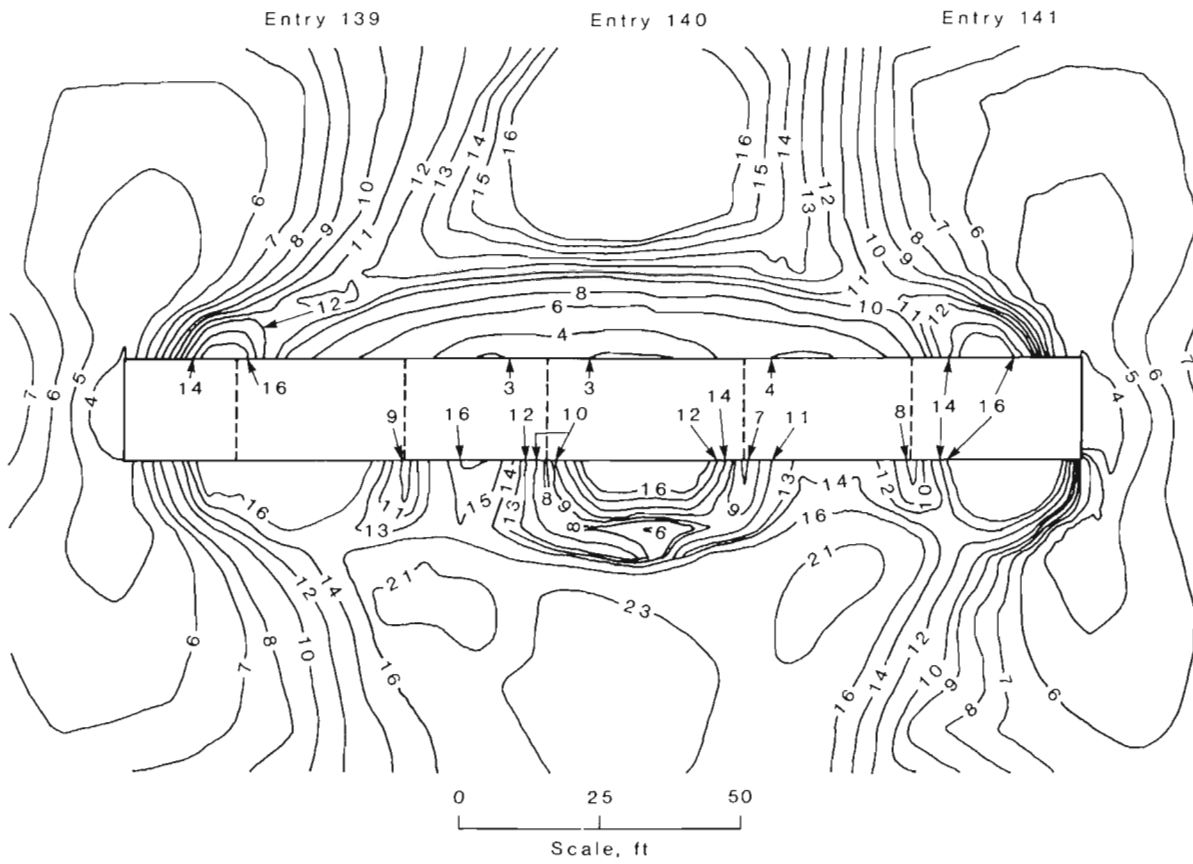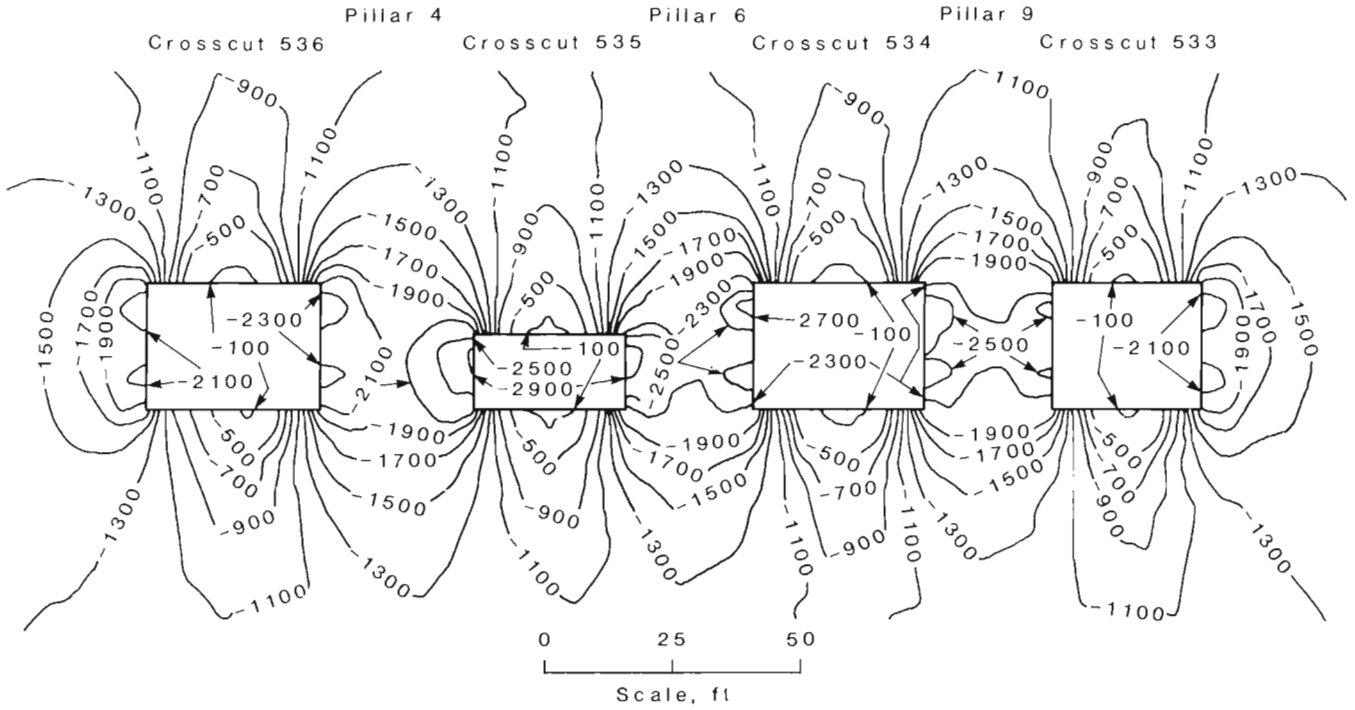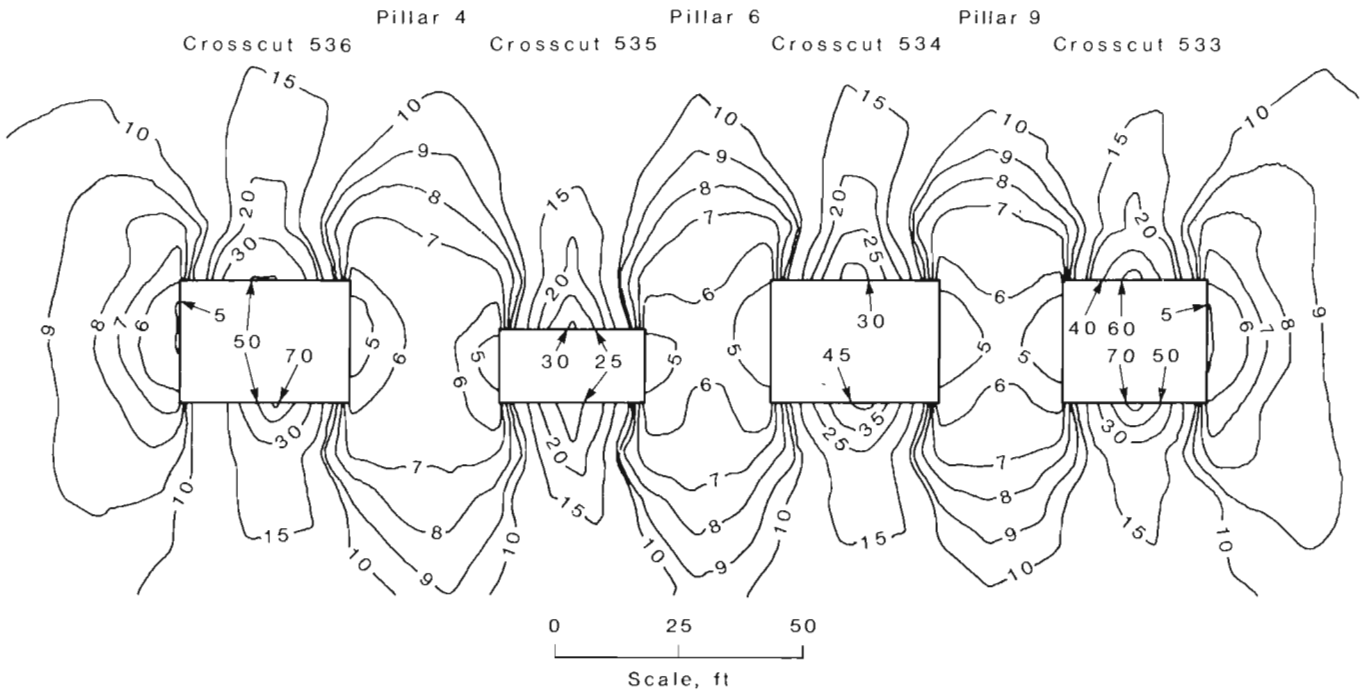Figure A–2.–East-west cross section of minor principal stress contours with entries removed, gravity load case.

Figure A—3.-East-west cross section of factor-of-safety contours with entries removed, gravity load case.

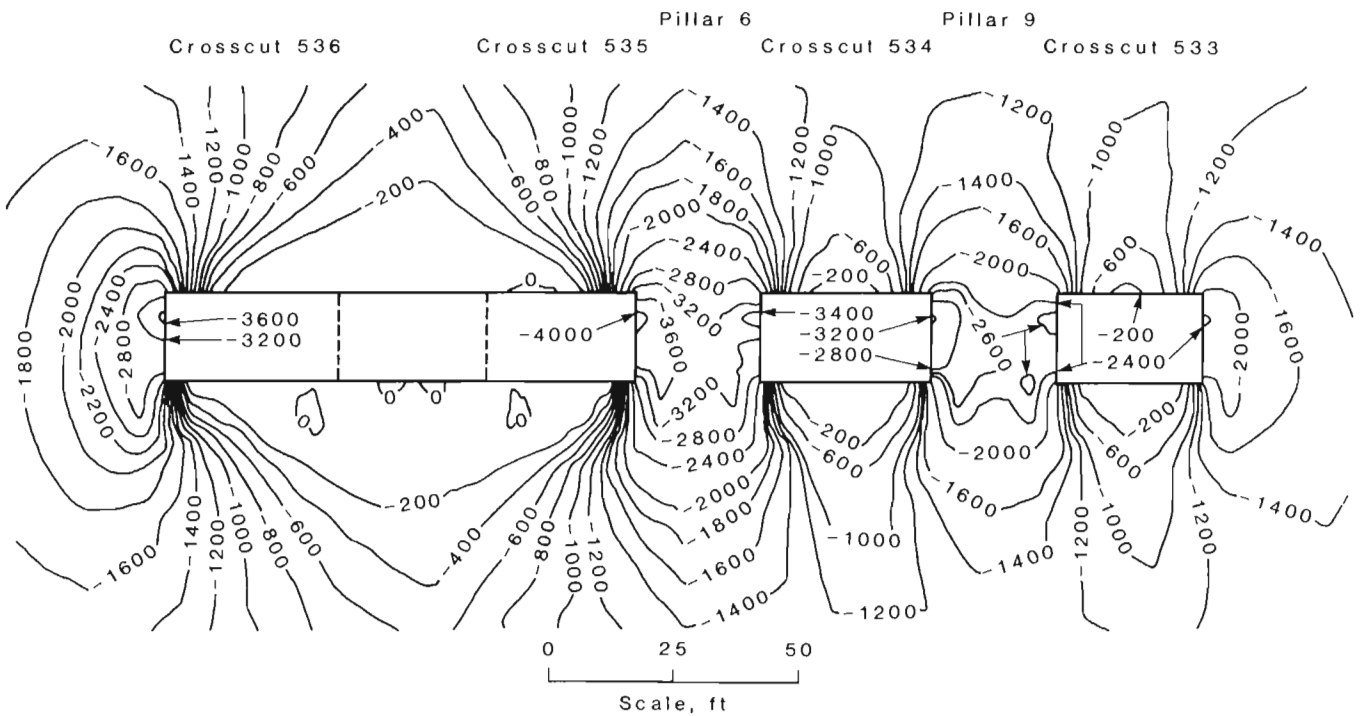Figure A—4.-East-west cross section of major principal stress contours with pillar 3 removed, gravity load case.

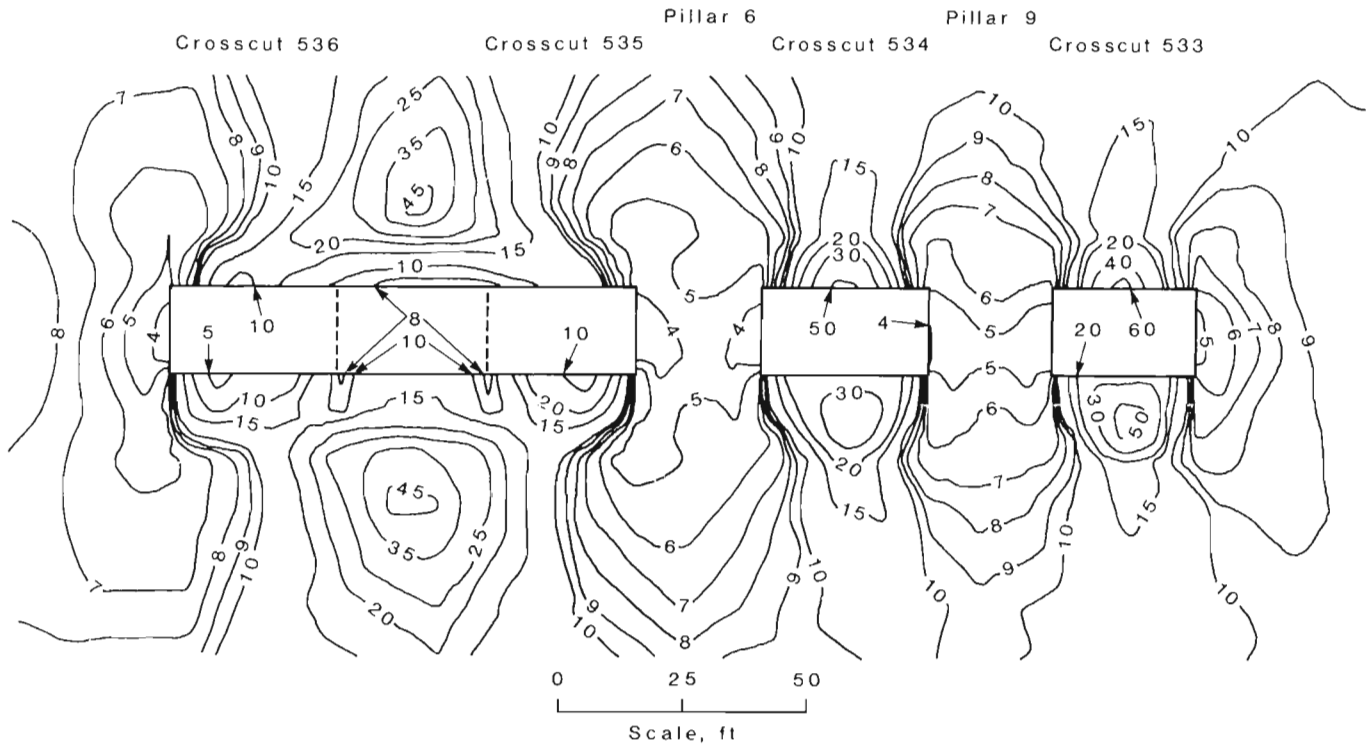**Figure A—5.-East-west cross section of minor principal stress contours with pillar 3 removed, gravity load case.**

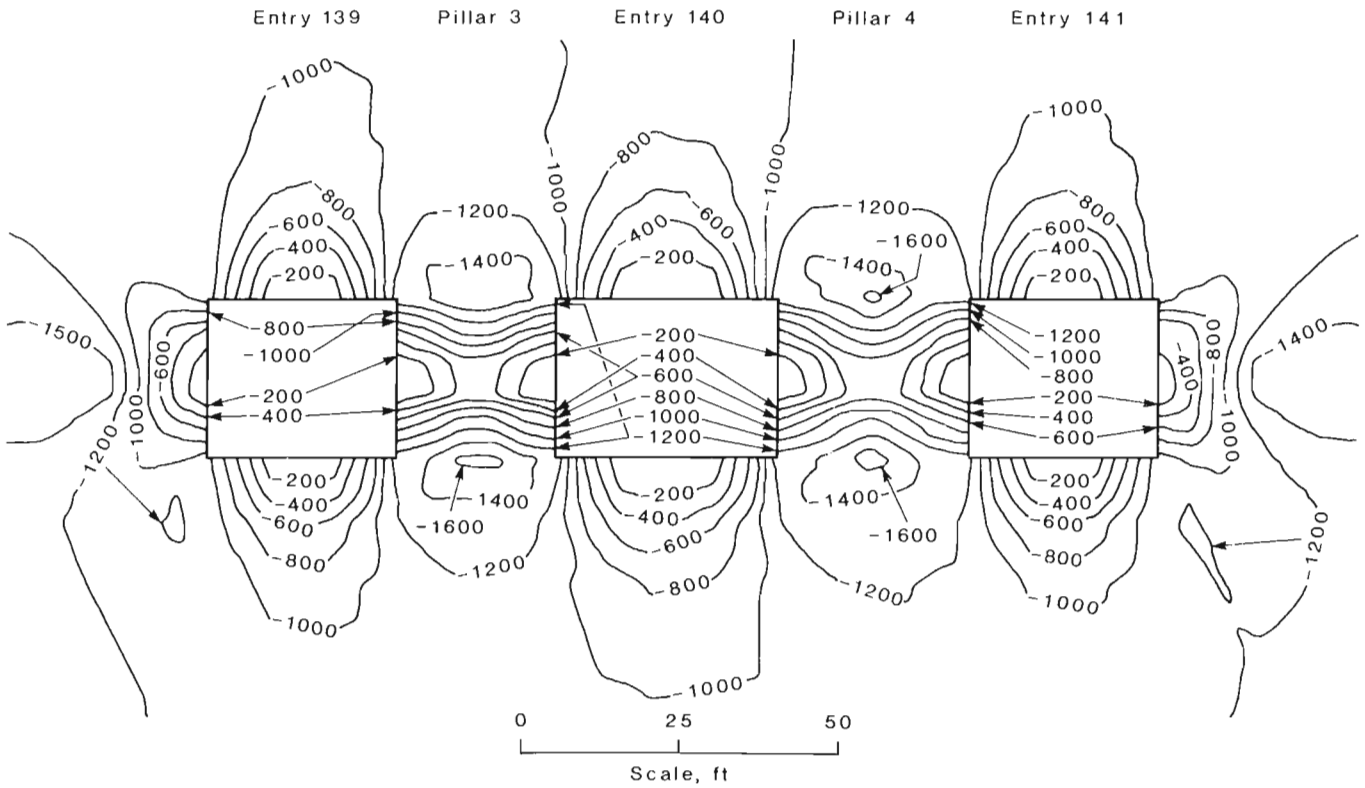**Figure A—6.-East-west cross section of factor-of-safety contours with pillar 3 removed, gravity load case.**
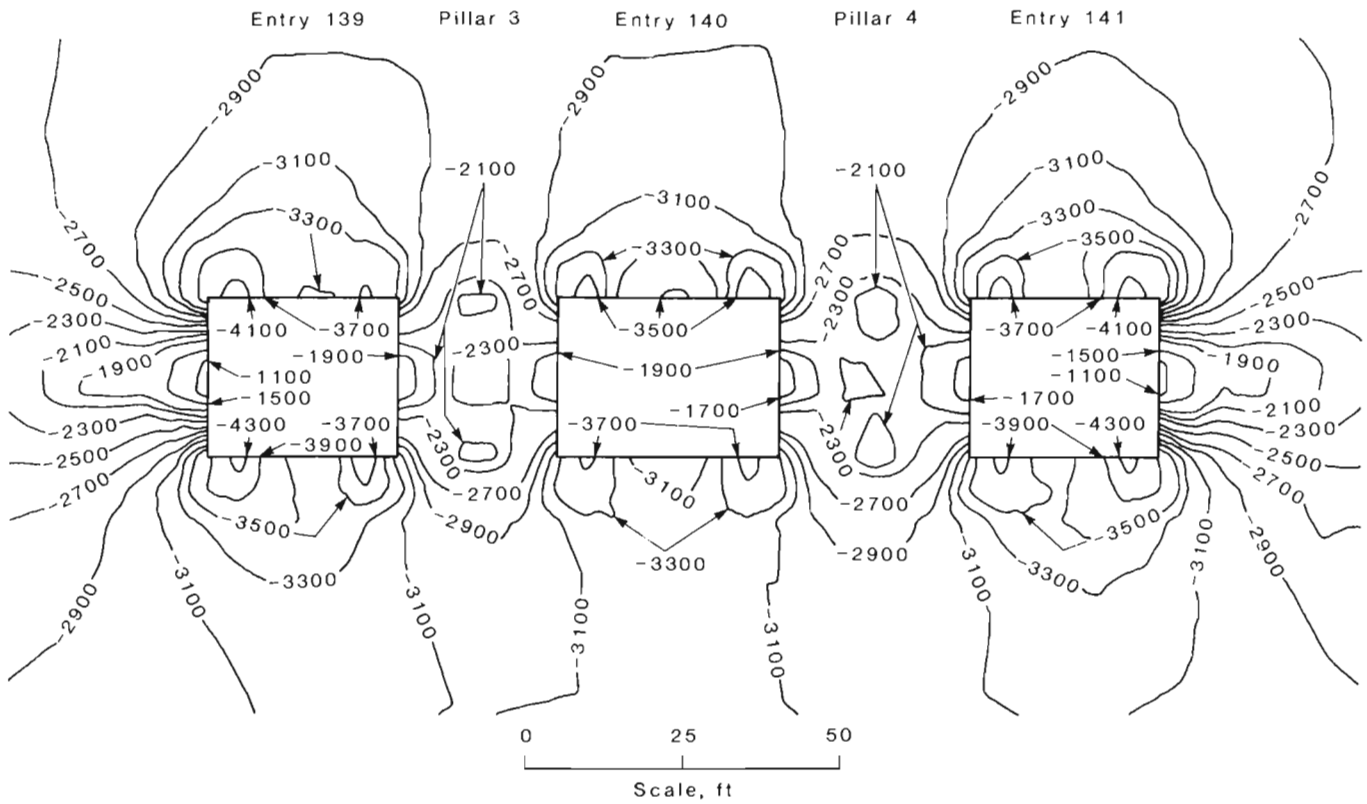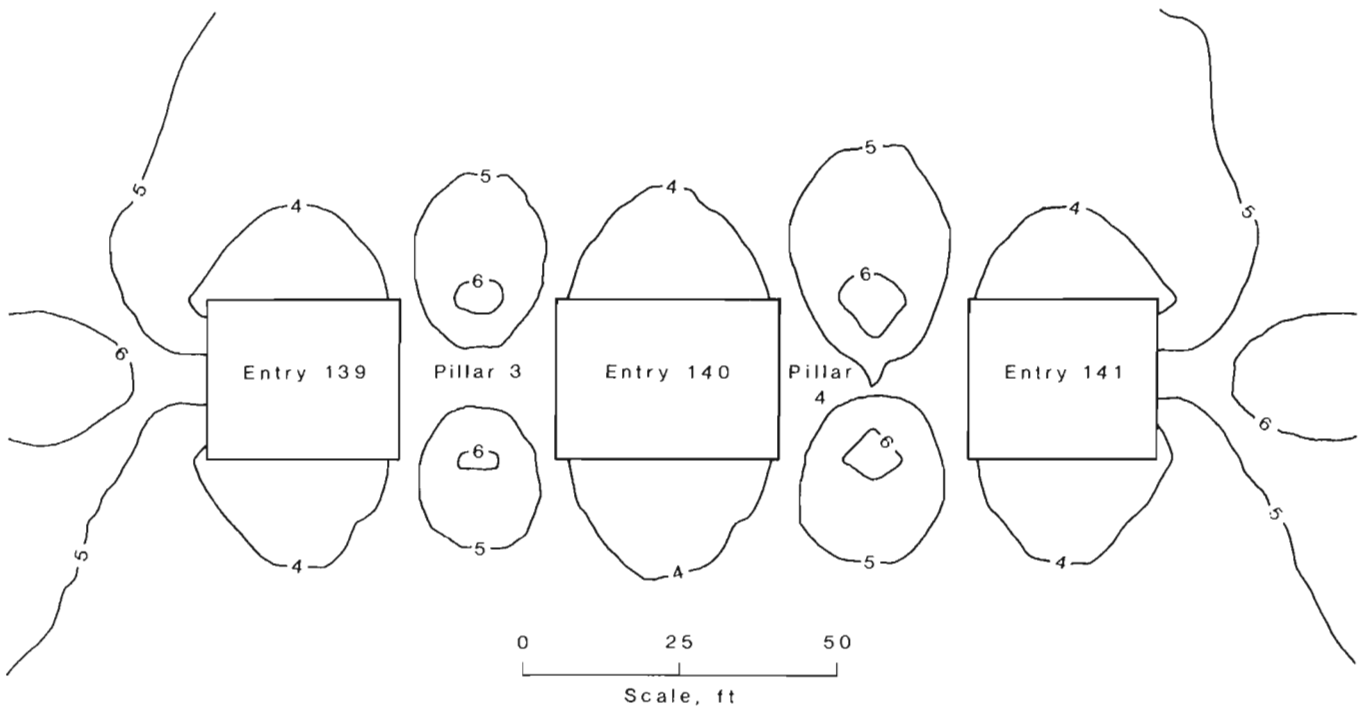
Figure A—7.-East-west cross section of major principal stress contours with pillars 3 and 4 removed, gravity load case.
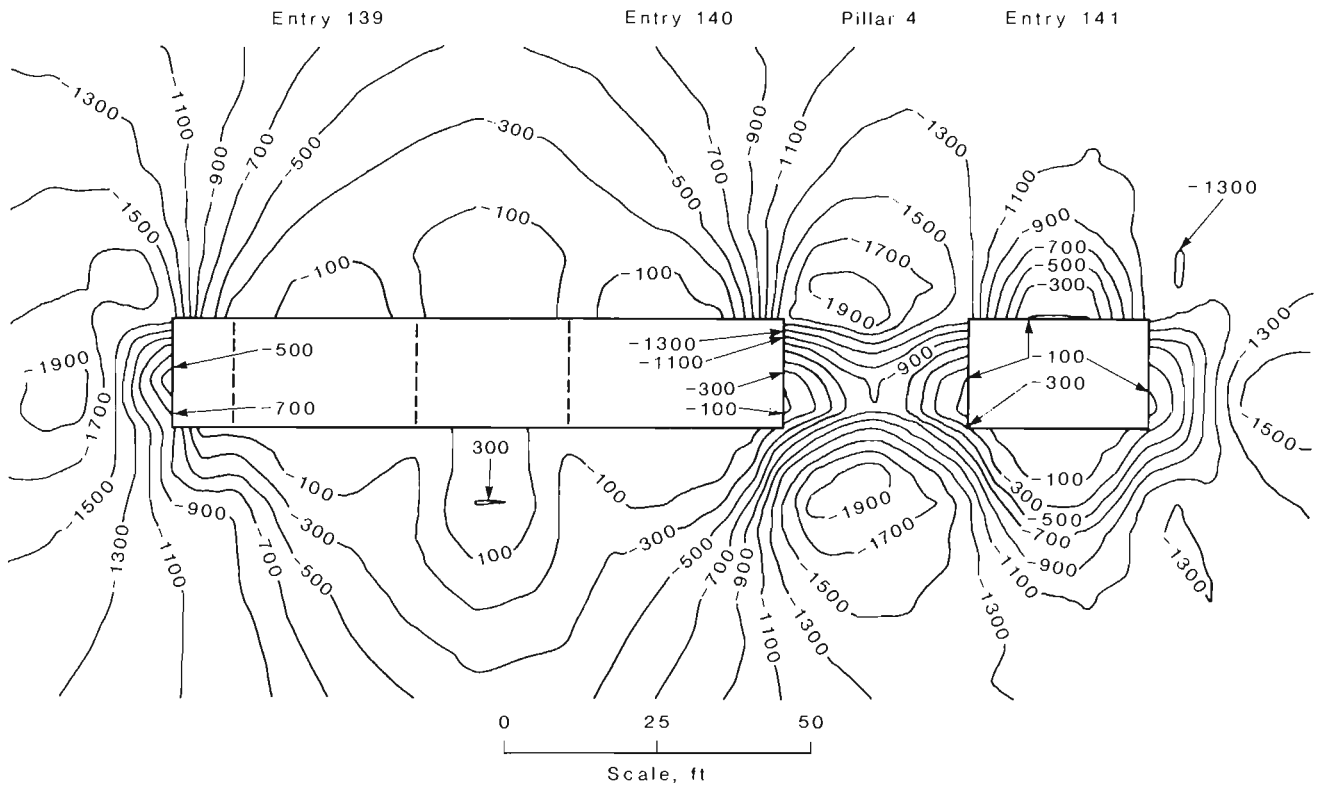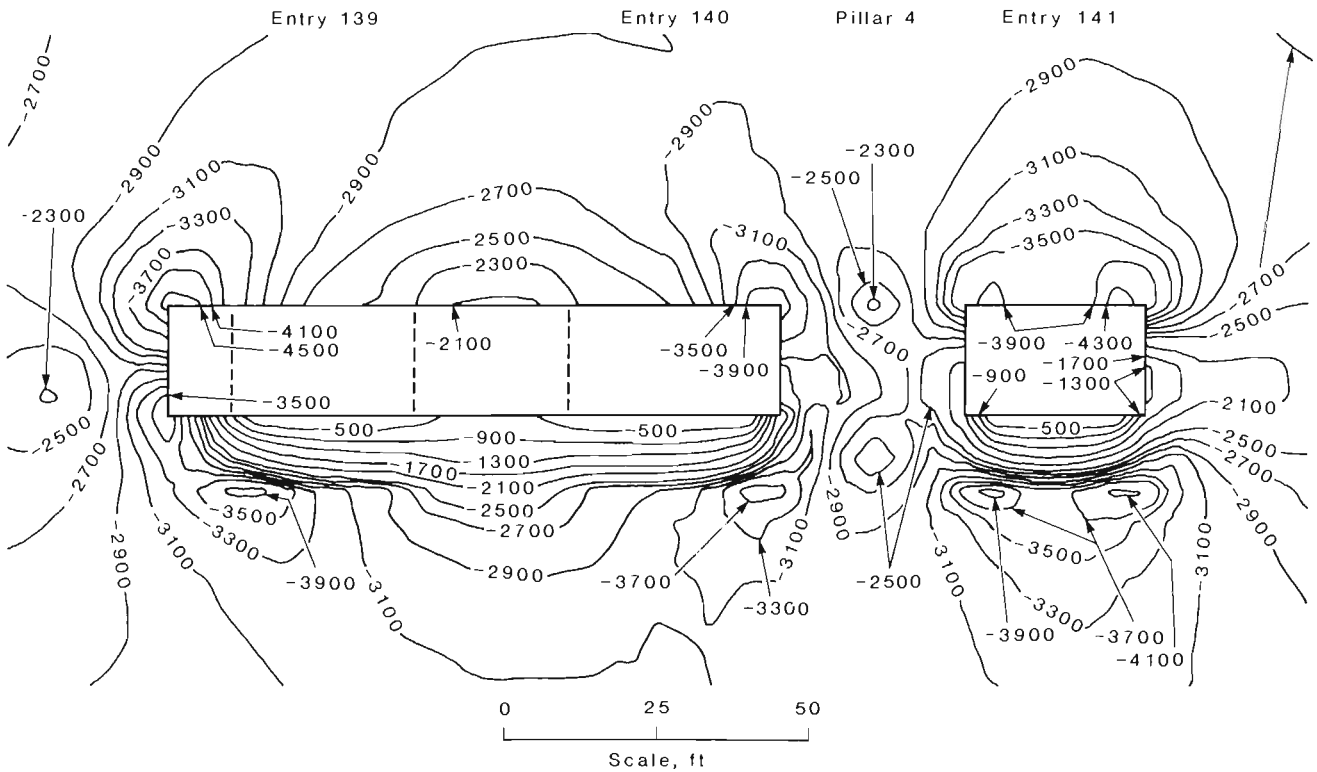

Figure A—8.-East-west cross section of minor principal stress contours with pillars 3 and 4 removed, gravity load case.

20

Figure A—9.-East-west cross section of factor-of-safety contours with pillars 3 and 4 removed, gravity load case.
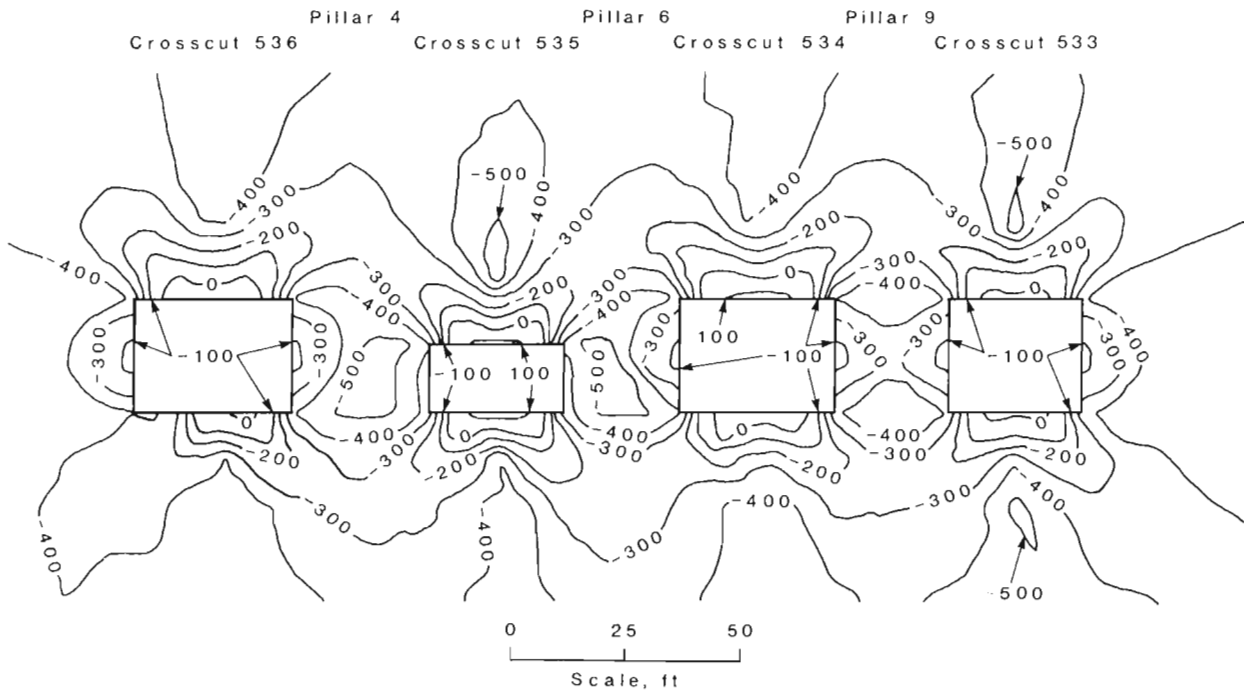
Figure A—10.-North-south cross section of major principal stress contours with crosscuts removed, gravity load case.

Pillar 4   Pillar 6   Pillar 9

Crosscut 536   Crosscut 535   Crosscut 534   Crosscut 533

0   25   50

Scale, ft

Figure A—11.-North-south cross section of minor principal stress contours with crosscuts removed, gravity load case.

Pillar 4   Pillar 6   Pillar 9

Crosscut 536   Crosscut 535   Crosscut 534   Crosscut 533

0   25   50

Scale, ft

Figure A—12.-North-south cross section of factor-of-safety contours with crosscuts removed, gravity load case.
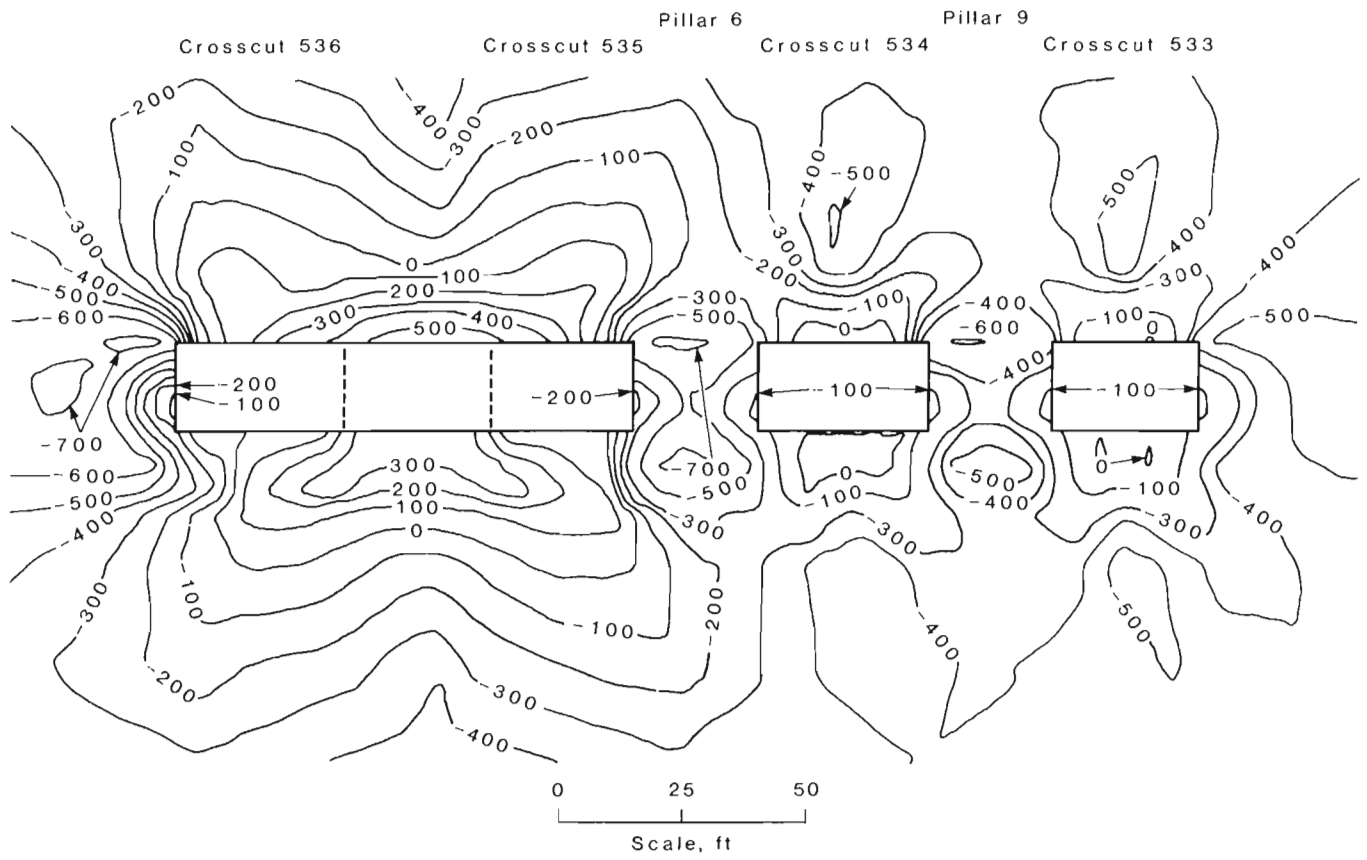
Figure A—13.-North-south cross section of major principal stress contours with pillar 4 removed, gravity load case.

Figure A—14.-North-south cross section of minor principal stress contours with pillar 4 removed, gravity load case.

Pillar 6   Pillar 9

Crosscut 536   Crosscut 535   Crosscut 534   Crosscut 533

0   25   50

Scale, ft

Figure A–15.-North-south cross section of factor-of-safety contours with pillar 4 removed, gravity load case.

Entry 139   Pillar 3   Entry 140   Pillar 4   Entry 141

0   25   50

Scale, ft

Figure A–16.-East-west cross section of major principal stress contours with entries removed, in situ load case.

24

Entry 139   Pillar 3   Entry 140   Pillar 4   Entry 141

Figure A—17.-East-west cross section of minor principal stress contours with entries removed, in situ load case.

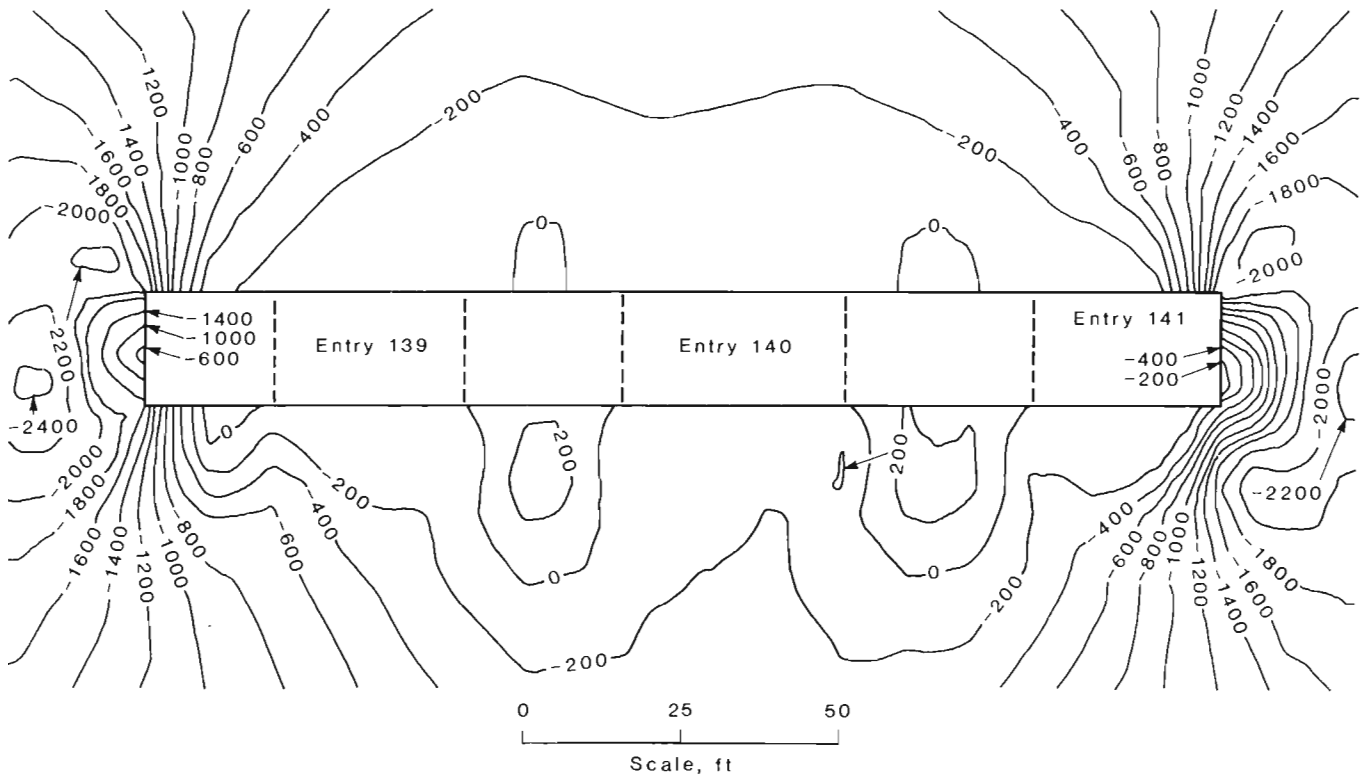Figure A—18.-East-west cross section of factor-of-safety contours with entries removed, in situ load case.

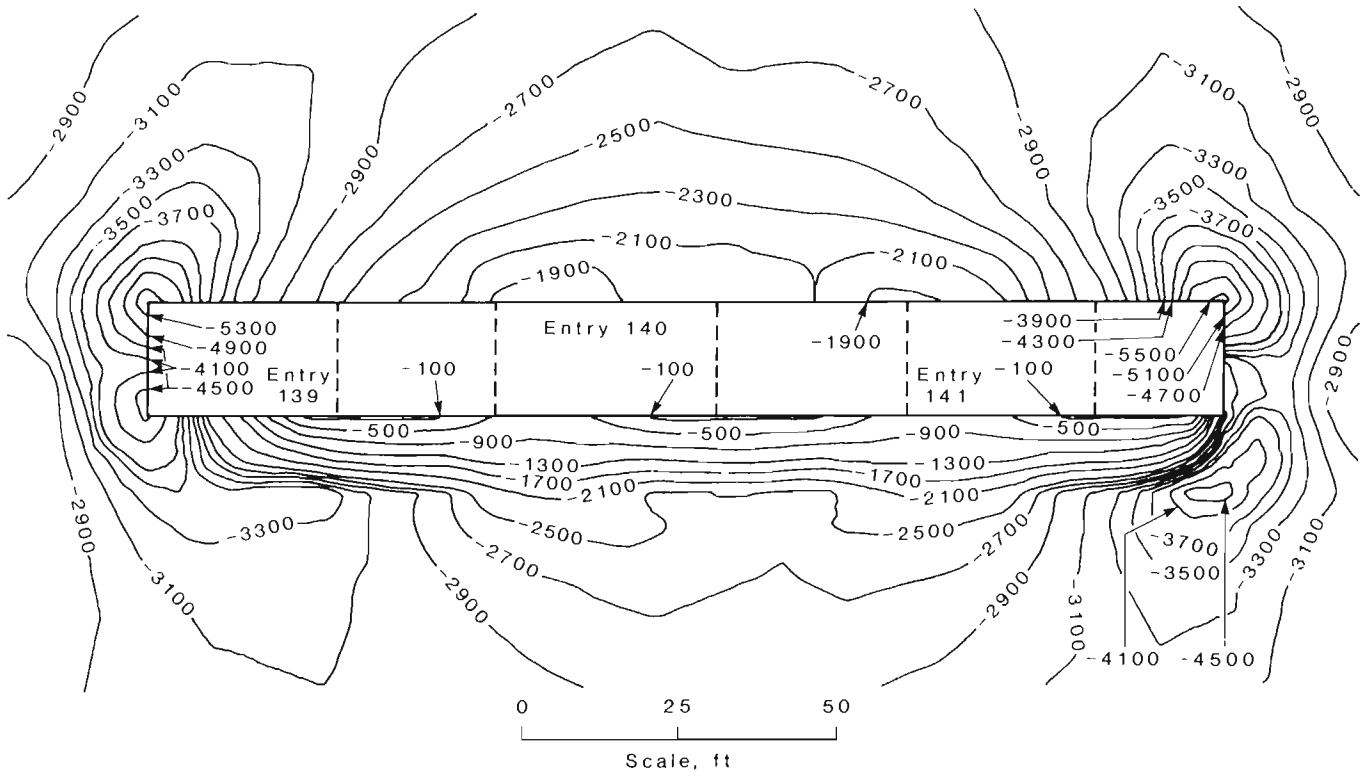Figure A—19.-East-west cross section of major principal stress contours with pillar 3 removed, in situ load case.

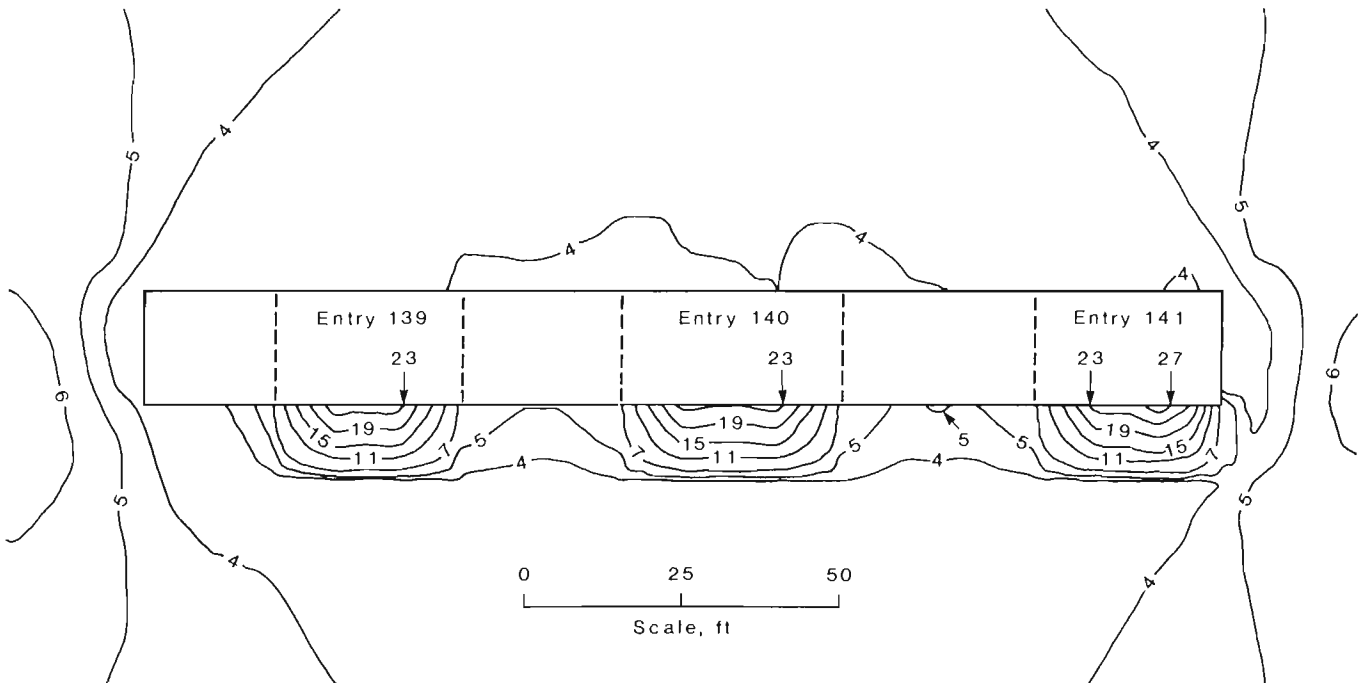Figure A—20.-East-west cross section of minor principal stress contours with pillar 3 removed, in situ load case.
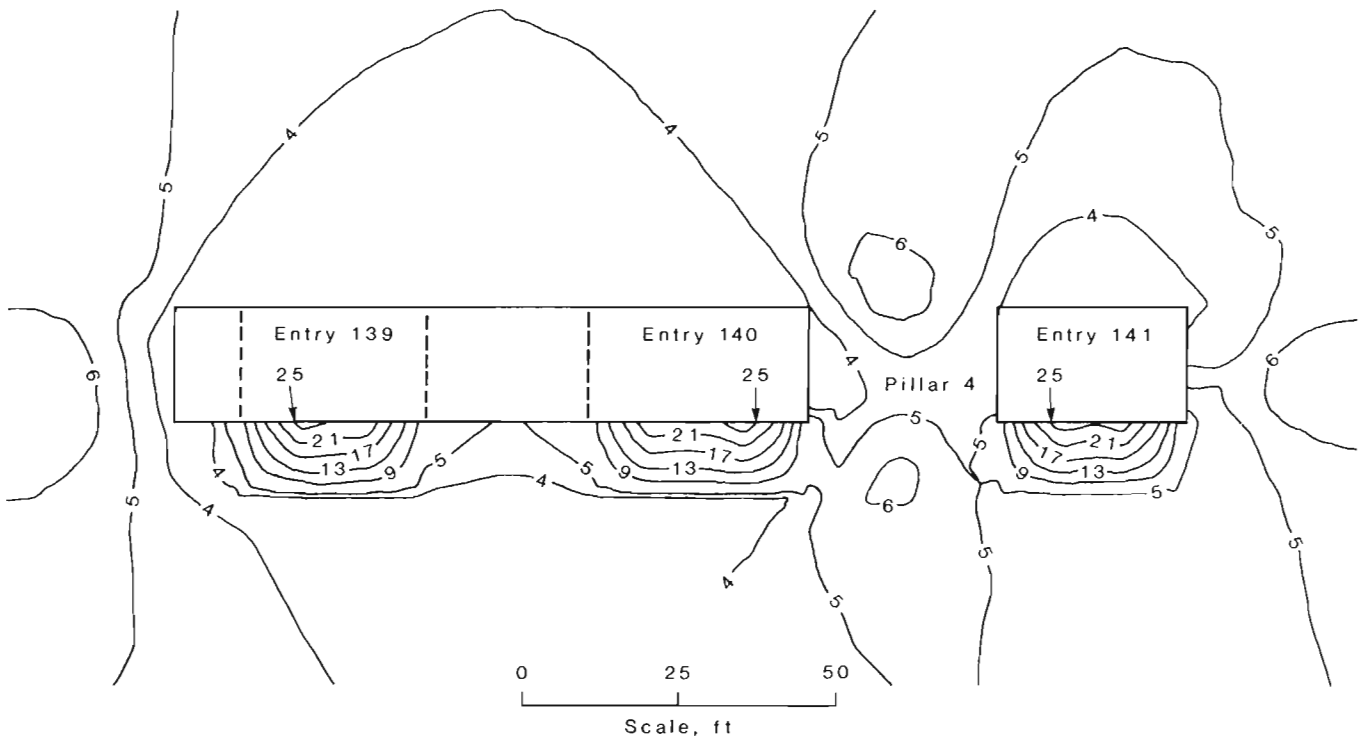
Figure A—21.-East-west cross section of factor-of-safety contours with pillar 3 removed, in situ load case.

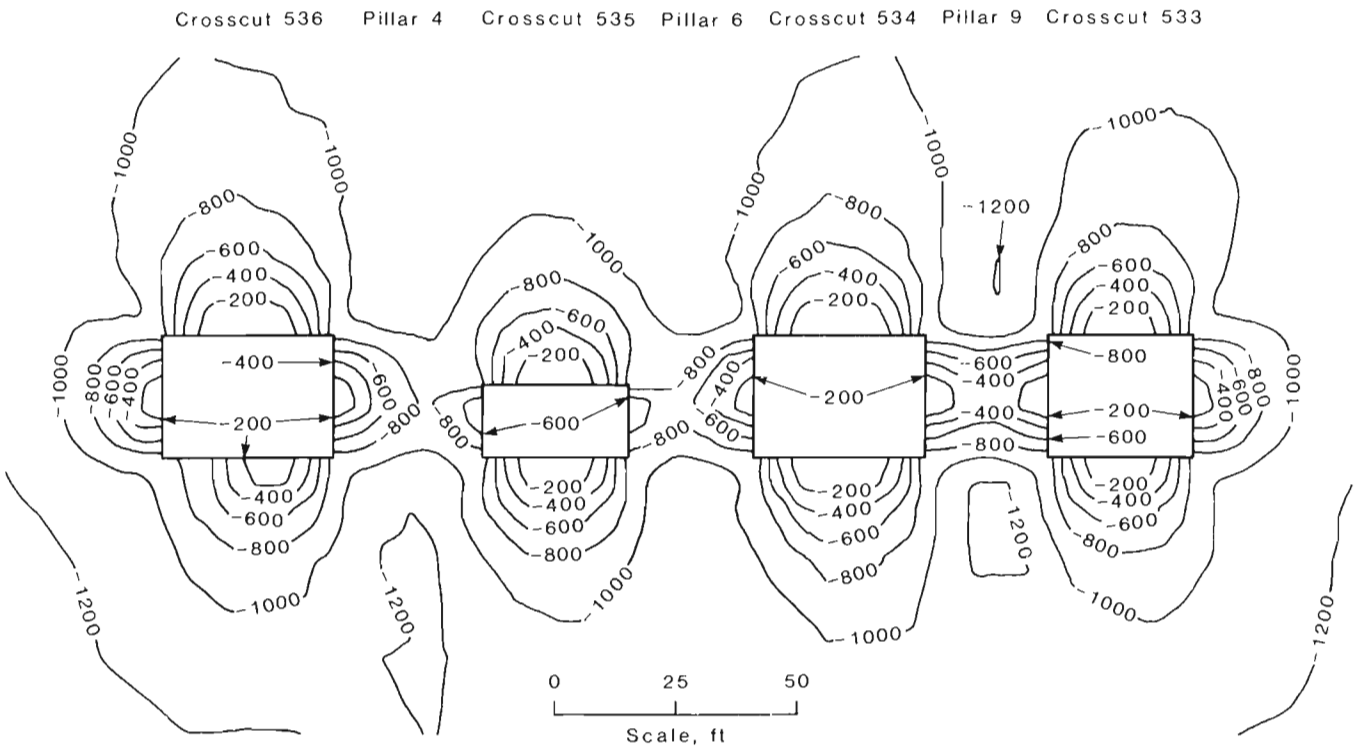Figure A—22.-East-west cross section of major principal stress contours with pillars 3 and 4 removed, in situ load case.
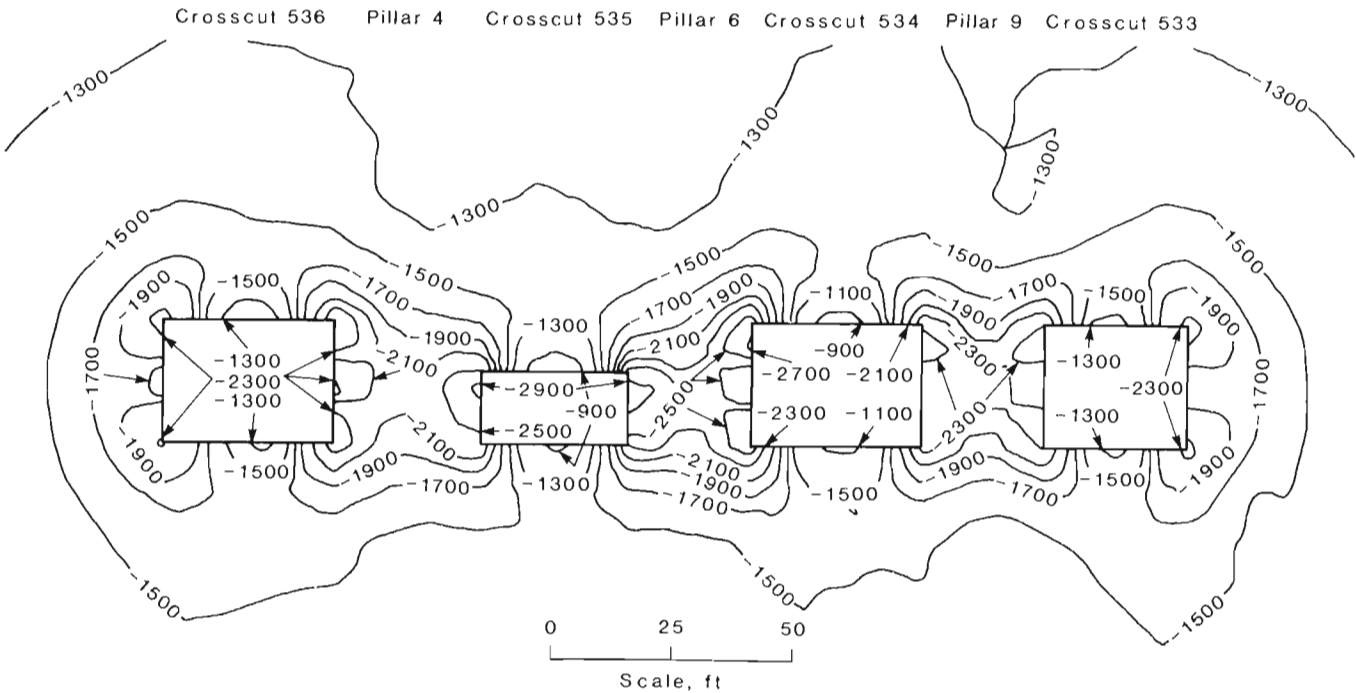
Figure A-23.-East-west cross section of minor principal stress contours with pillars 3 and 4 removed, in situ load case.

Figure A-24.-East-west cross section of factor-of-safety contours with pillars 3 and 4 removed, in situ load case.

Crosscut 536   Pillar 4   Crosscut 535   Pillar 6   Crosscut 534   Pillar 9   Crosscut 533

Figure A–25.–North-south cross section of major principal stress contours with crosscuts removed, in situ load case.

Crosscut 536   Pillar 4   Crosscut 535   Pillar 6   Crosscut 534   Pillar 9   Crosscut 533

Figure A–26.–North-south cross section of minor principal stress contours with crosscuts removed, in situ load case.
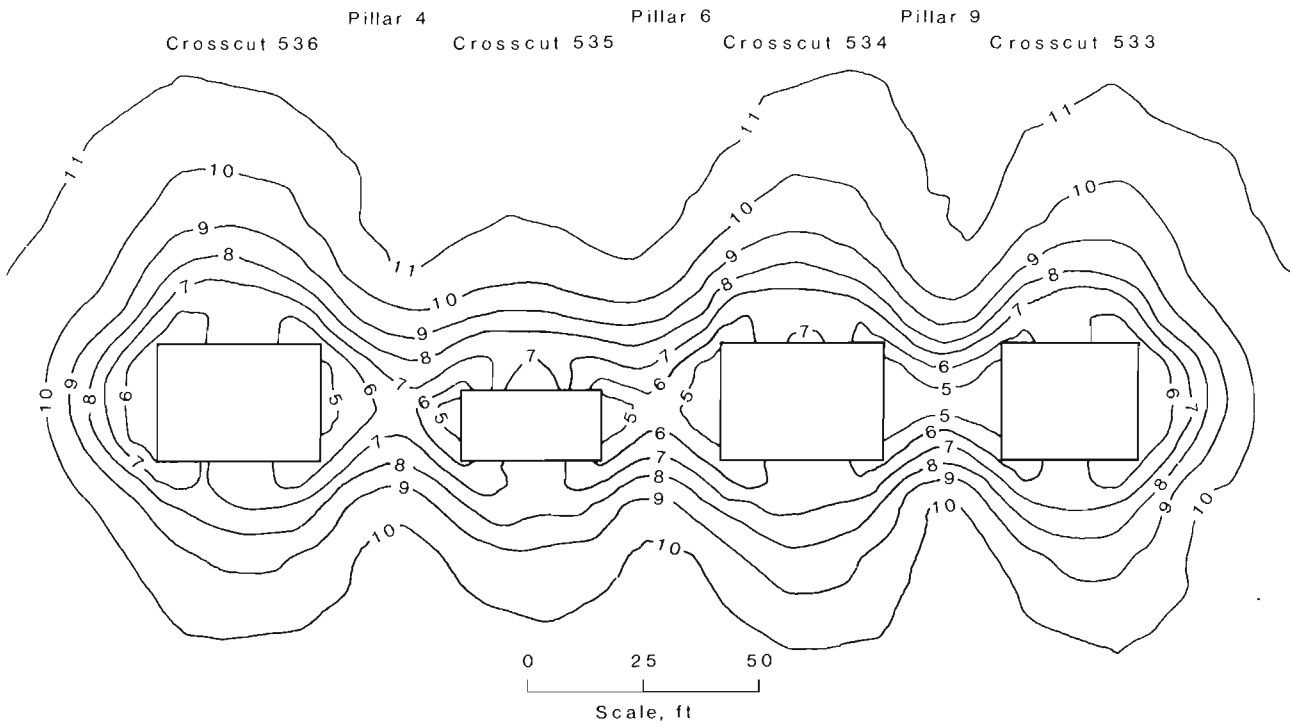
Figure A—27.-North-south cross section of factor-of-safety contours with crosscuts removed, in situ load case.
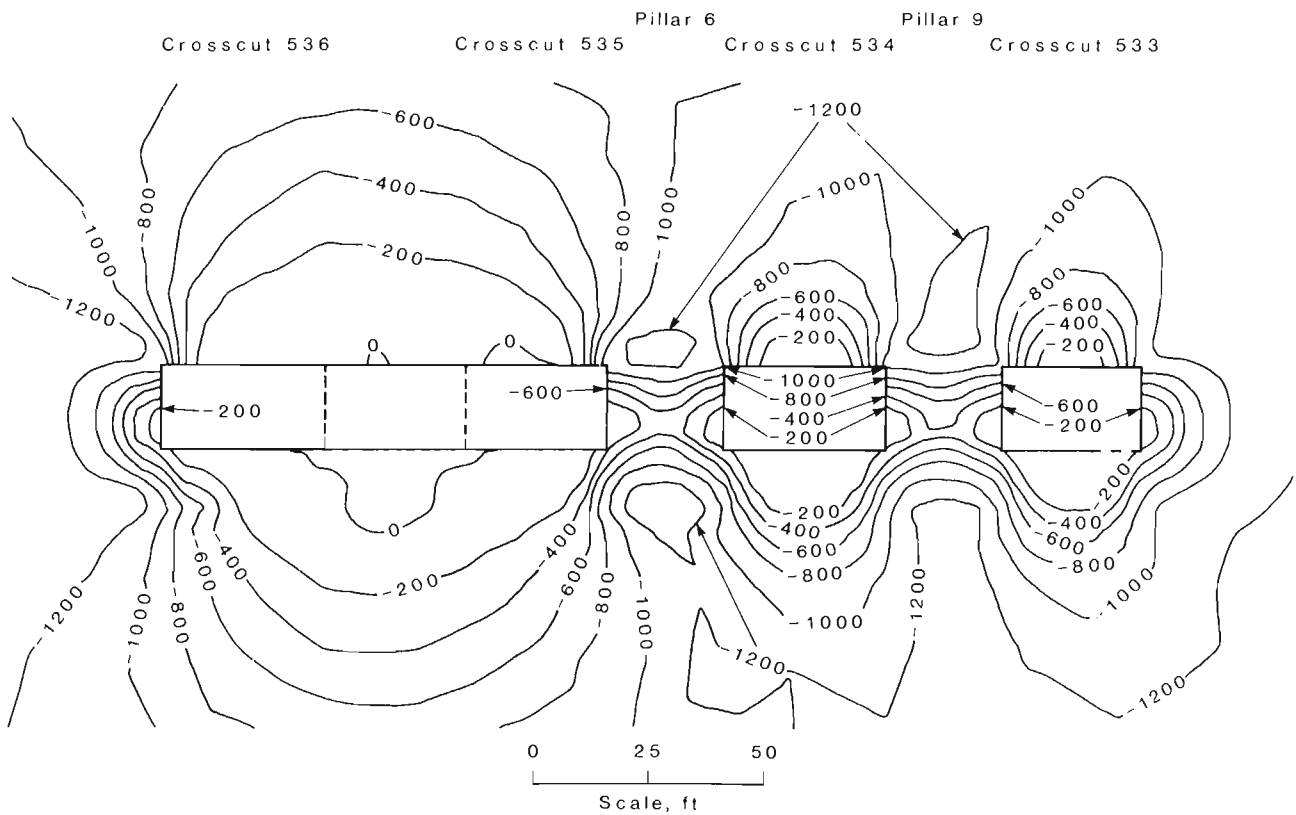
Figure A—28.-North-south cross section of major principal stress contours with pillar 4 removed, in situ load case.
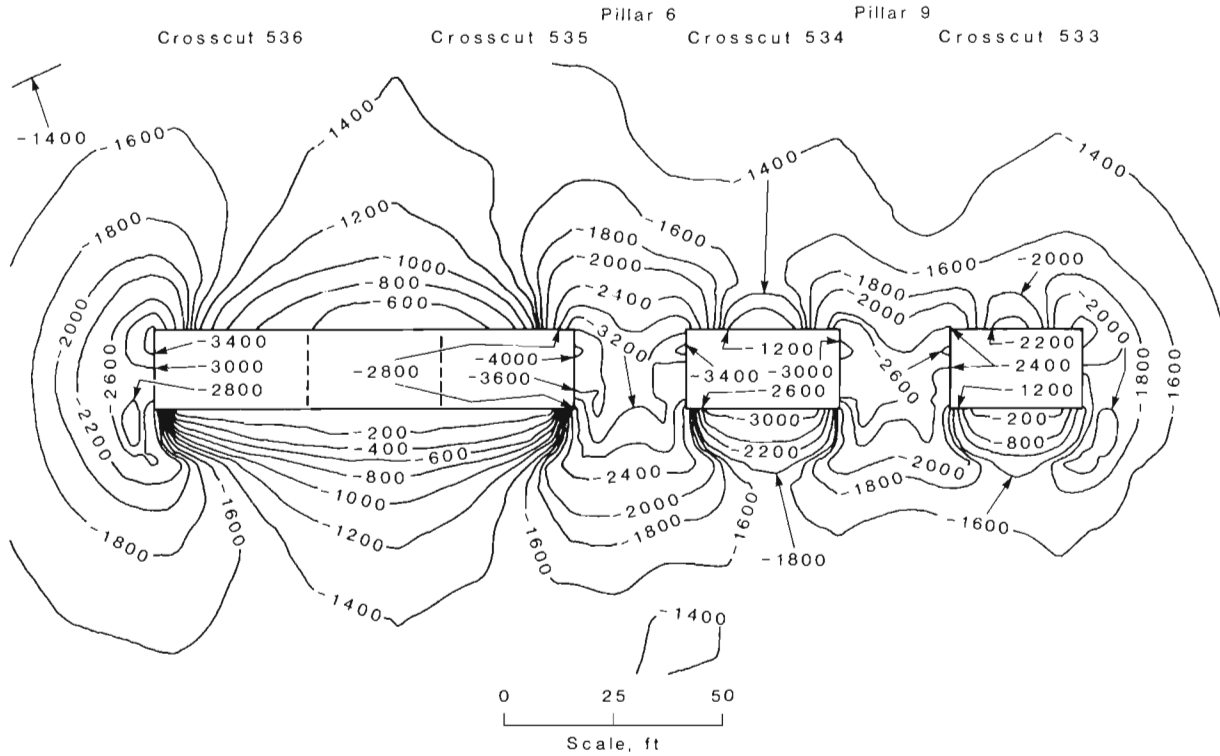
Figure A–29. North-south cross section of minor principal stress contours with pillar 4 removed, in situ load case.
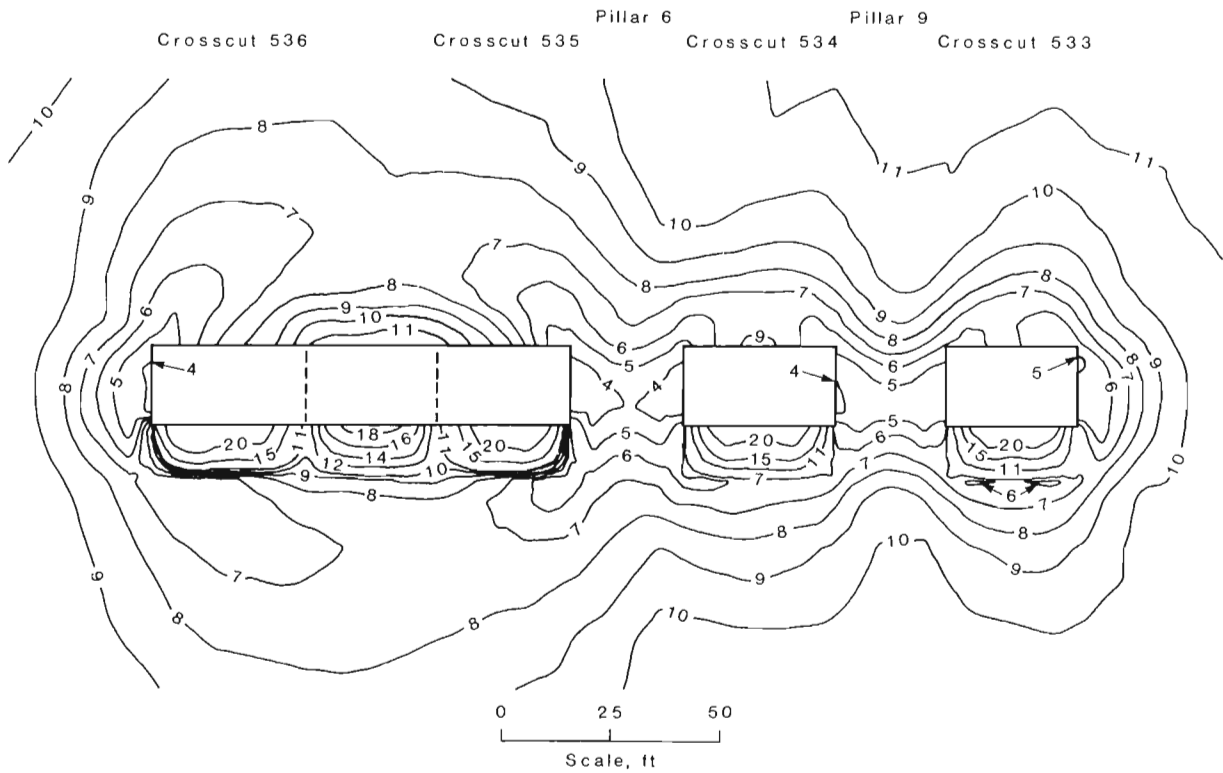
Figure A–30. North-south cross section of factor-of-safety contours with pillar 4 removed, in situ load case.